CHALMERS
UNIVERSITY OF TECHNOLOGY

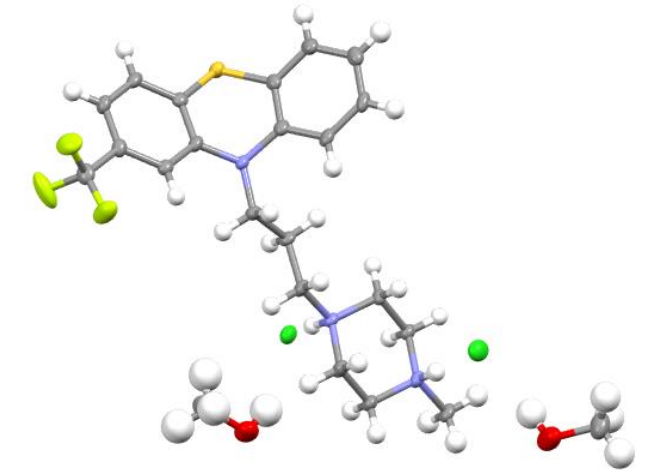

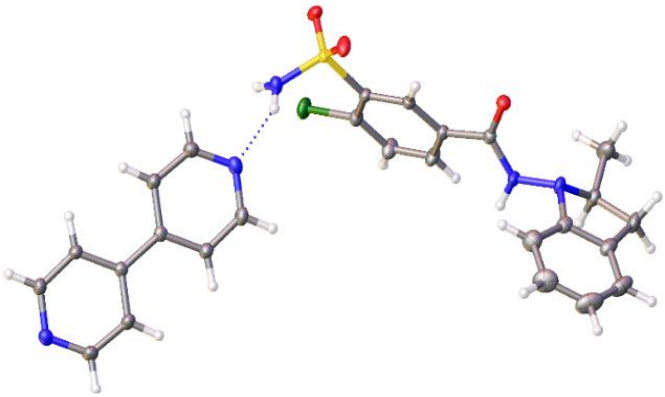

Cocrystal Screening for Indapamide and Trifluoperazine

Resulting in the Cocrystal Indapamide:4,4-bipyridine, Trifluoperazine Salt Solvate, and a Cocrystal Including Decomposed Indapamide.

Master's Thesis in Solid State Chemistry

SANNA LARSSON
In collaboration with Okky Putra, Francoise Mystere Amombo Noa, Philip Corner, Lars Öhrström

DEPARTMENT OF CHEMISTRY AND CHEMICAL ENGINEERING
CHALMERS UNIVERSITY OF TECHNOLOGY

Gothenburg, Sweden 2022
www.chalmers.se

Abstract

Trifluoperazine and indapamide are active pharmaceutical ingredients (APIs). Trifluoperazine is an antipsychotic and an antiemetic, while indapamide is effective against high blood pressure and is also a diuretic. They are both hygroscopic, which is a physiochemical property dependent on the crystal structure of the compounds. The crystal structure can be changed by creating polymorphs or multicomponent crystals. An attempt was made to find multicomponent crystals, specifically cocrystals, of either of the APIs trifluoperazine and indapamide, and characterize any cocrystals found. The goal of this was to alter the hygroscopicity of the APIs, preferably to a lower hygroscopicity. The chosen method was to use COSMOtherm to theoretically compute the excess enthalpy of different combinations of the APIs and potential coformers. The combinations with lowest excess enthalpy, was then prioritized for cocrystal screening with powder x-ray diffraction (PXRD). Different methods such as liquid assisted grinding (LAG) and isothermal slurry conversion were used to combine the APIs with the potential coformers. Promising combinations where a new PXRD pattern was formed, were produced through isothermal slurry conversion in larger amounts of 500-700mg. The resulting materials were dried and used in evaporative cocrystallization, with an array of different solvents. Evaporative cocrystallization resulted in many cases of crystals, which were analyzed through single crystal x-ray diffraction (SCXRD) when the crystal quality allowed. This resulted in finding the cocrystal **indapamide:4,4-bipyridine** (1:1) and one trifluoperazine salt solvate. The trifluoperazine salt solvate is **trifluoperazine:methanol:chloride** (1:2:2). A cocrystal hydrate including the previously unknown molecule **N-isopropyl-2-methyl-indolin-1-amine** was also found. N-isopropyl-2-methyl-indolin-1-amine is the result of decomposed indapamide and the cocrystal including this compound is **1,5-naphthalenedisulfonic acid: N-isopropyl-2-methyl-indolin-1-amine:H_2O** (2:1:2). Characterization of **indapamide:4,4-bipyridine** showed significantly reduced hygroscopicity compared to both the API and the coformer.

Table of Contents

Acronyms and Abbreviations

Acronym	Expansion of Acronym
API	Active Pharmaceutical Ingredient
DSC	Differential Scanning Calorimetry
DVS	Dynamic Vapor Sorption
PXRD	Powder X-Ray Diffraction
RH	Relative Humidity
SCXRD	Single Crystal X-Ray Diffraction
TGA	Thermogravimetric Analysis
v/v	Volume per Volume
w/w	Weight per Weight

Abbreviation of chemical name	Chemical name
ACN	Acetonitrile
BPD	4,4-bipyridine
EAM	Etidronic acid monohydrate
EtOH	Ethanol
GA	Gallic acid
IND	Indapamide
IMIA	N-isopropyl-2-methyl-indolin-1-amine
MeOH	Methanol
NDS	1,5-Naphthalenedisulfonic acid
NDST	1,5-Naphthalenedisulfonic acid tetrahydrate
OA	Oxalic acid
TFP	Trifluoperazine
THF	Tetrahydrofuran

Introduction

The physiochemical properties of an active pharmaceutical ingredient (API) depend on its crystal structure. Examples of important physiochemical properties of APIs are stability, solubility, bioavailability and hygroscopicity. The latter, hygroscopicity, can be an issue, where the API might absorb excessive water or deliquesce during storage or processing. The physiochemical properties of an API can be modified by changing the crystal structure of the compound. This can be done by changing crystal structure using two different approaches: change to different crystal form or polymorph, and creating a multicomponent crystal. A polymorph has the same molecular formula as the original API but can have different conformation in the crystal, a different molecular arrangement, or a combination thereof. Multicomponent crystals can be classified into hydrates, solvates, salts, cocrystals, and combination thereof. (Christer B. Aakeröy, 2018) This thesis was an attempt in finding new crystal structures of APIs of trifluoperazine and indapamide, respectively, with a focus on creating cocrystals. Trifluoperazine is an antipsychotic and an antiemetic (National Center for Biotechnology Information, 2022a), while indapamide is effective against high blood pressure and is also a diuretic. (National Center for Biotechnology Information, 2022b) Trifluoperazine and indapamide were chosen for this thesis as they are both hygroscopic APIs, relatively inexpensive and had few already known multicomponent crystals.

The starting-point of this thesis was a theoretical prediction on which coformers (cocrystal former) are likely to form cocrystals with trifluoperazine and indapamide respectively using excess of enthalpy calculation. The screening of cocrystal was subsequently performed using slurry and liquid assisted grinding (LAG) methods. For all combinations likely to form cocrystals, there was an attempt to grow crystals of the cocrystal through slow evaporation using an array of different solvents. All crystals formed were analyzed with single crystal X-ray diffraction (SCXRD). The hygroscopicity was characterized using isothermal vapor sorption analysis, more specifically dynamic vapor sorption (DVS).

Aim

The aim of this research was to find multicomponent crystals, preferably cocrystals, including either of the pharmaceutically active ingredients (API) trifluoperazine or indapamide, and characterize the crystals found. The goal of this study was to alter the hygroscopicity of an API, as a change in structure can lead to a change of physiochemical properties, preferably to a lower hygroscopicity.

Limitations

As experimental screening of cocrystals takes a lot of time; limits were needed to make the project feasible. Two hygroscopic crystalline APIs, were chosen for the attempt of making cocrystals. The project did not include work with amorphous pharmaceutical materials, only crystalline APIs and coformers. When screening for coformers to form cocrystals, only pharmaceutically acceptable coformers were considered.

Theory

Hygroscopicity

Hygroscopicity describes water vapor uptake in solids and the ability of a solid to take up and retain water. It can be defined by the following: “rate and extent of water vapor uptake by a solid at certain relative humidity (RH) values and temperatures”. (Dabing Chen, 2009) The reason that hygroscopicity in pharmaceutical solids is important is that their physicochemical properties can be altered when they take up water. Water sorption can thus negatively affect product performance. For drug candidates that do not form stable hydrates, the hygroscopicity criterion is that at $25^{\circ}C$, 60% RH water uptake should be less than 2% w/w, and definitely not more than 5% w/w. (Dabing Chen, 2009) Hygroscopicity depends upon water-solid interactions. The main modes of water uptake into a solid are surface adsorption, absorption and liquefaction. (Ann W. Newman, 2008) Other modes of water-solid interactions are capillary condensation and hydrate formation. (Dabing Chen, 2009)

Crystalline and Amorphous Structure

Solid materials can be divided into crystalline and amorphous materials. In a crystalline material the atoms are arranged in a periodic lattice. A single crystal is a perfect lattice of atoms, with no defects. However, many solids are polycrystalline. This means that they are composed of small crystalline grains. In a polycrystalline material the number of atoms in a perfect crystalline environment is still much larger than the number of atoms on the grain boundary. Solids that are not crystalline are amorphous, which means that there is no long-range order. (Hofmann, 2015) It is worth noting that amorphous materials take up significantly more water than their crystalline counterparts. (Dabing Chen, 2009)

Crystallinity means that a basis, the building block of a crystal, is being arranged in a lattice. (Hofmann, 2015) In three dimensions a lattice can be defined as all points that can be reached by three-dimensional vectors $\vec{R}$, created from linear combination of the three base vectors $\overrightarrow{a_1}$, $\overrightarrow{a_2}$, $\overrightarrow{a_3}$ as

$$\vec{R} = m\overrightarrow{a_1} + n\overrightarrow{a_2} + o\overrightarrow{a_3}$$

This is the Bravais lattice where m, n, o are any integers and the lengths of vectors $\overrightarrow{a_1}$, $\overrightarrow{a_2}$, $\overrightarrow{a_3}$ are the lattice constants. In a crystal the basis, which is on the lattice points, can consist of one or several atoms, or complex molecules. A crystal has both translational symmetry and point symmetry. (Hofmann, 2015)

X-ray diffraction

The most important technique for determining crystal structure is X-ray diffraction. As X-rays interact weakly with matter, it can be assumed that X-rays going into a sample are diffracted once at most. (Hofmann, 2015) This is called the kinematic approximation. Assuming that the X-ray source and detector are very far from the sample enables the assumption that ingoing and outgoing waves can be treated as plane waves. X-ray diffraction into crystal planes is described by Bragg theory. The construction for the derivation of the Bragg condition can be seen in the figure below (Hofmann, 2015)

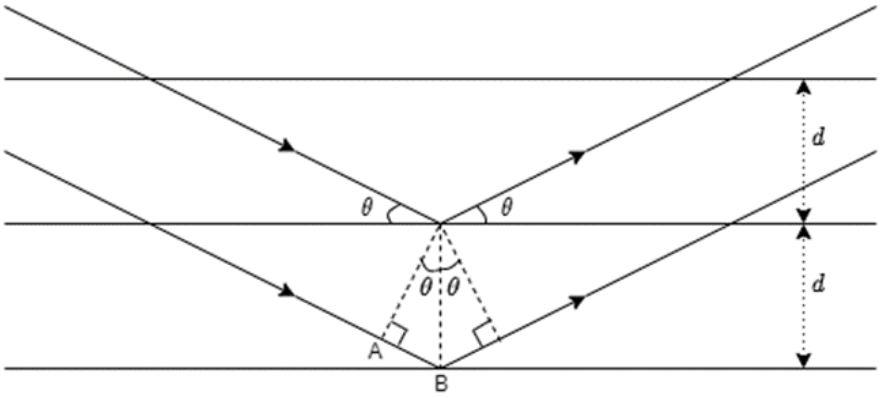

Figure 1: Construction for derivation of Bragg condition. d is the interplanar distance between crystal planes and θ is the angle between X-rays and the crystal planes. 2θ is the change in direction between the incoming and the outgoing waves. Picture adapted from schematic in "Solid State Physics: An Introduction" (Hofmann, 2015)

The condition for constructive interference for the outcoming waves is that $2 \cdot AB = n \cdot \lambda$, where AB is the distance between A and B, d is the interplanar distance, λ is the wavelength and n is any natural number. As $AB = d \cdot \sin\theta$, this result in the Bragg condition for constructive interference (Hofmann, 2015)

$$n \cdot \lambda = 2 \cdot d \cdot \sin\theta \;\Rightarrow\; \theta = \sin^{-1}\frac{n\lambda}{2d}$$

PXRD

Powder X-ray diffraction (PXRD) is is a technique used to verify and prove the identity of new phases and compounds as a unique PXRD pattern is shown for every complex due to its structural features. It operates under the assumption that the individual grains in the powder will be randomly arranged, making all planes and corresponding interplanar distances of the sample represented in the X-ray diffraction. (Speakman, 2022) As each individual lattice structure will have different dimensions, the resulting diffractogram of intensity by θ acts as a fingerprint for identifying different structures. This means that if two powders are mixed without cocrystallization or reacting, meaning a physical mixture, the PXRD pattern will look like an overlay of the PXRD patterns of the two individual powders. If a new structure has been formed, there will instead be a new PXRD pattern.

SCXRD

Single-crystal X-ray diffraction (SCXRD) is an analytical technique that provides information about the lattice structure of a crystalline material. The sample used should be an optically clear, unfractured single crystal of the crystalline material which is about 30-300µm in size. It is ideal if the size is about 150-250µm. Examples of lattice structure information that can be found is unit cell dimension, bond-lengths, bond-angles and details of site-ordering. SCXRD works through X-rays being generated from a cathode ray tube, filtered to be monochromatic, collimated to become concentrated, and then directed at the sample. The X-rays are diffracted by the sample, as described by Bragg's law. A charge-coupled device (CCD) is a detector which transform the diffracted X-ray photons into an electrical signal which is then sent to a computer for processing. By changing the geometry of the incoming X-rays, the orientation of the centered crystal and the detector, all possible diffraction directions of the lattice are attained. The changes in direction for the diffracted waves compared to the incident waves are recorded, as they contain information about the structure. (Dutrow, 2022) Single-crystal refinement is when the data generated from the X-ray analysis is refined to obtain a better crystal structure. In single-crystal refinement the collected data is used to create an electron density map, where elements can be assigned to density centers. Often trial and error is necessary to make the right assignment. After correct assignments of elements, refinement is done cyclically. In each cycle small changes are made to the structure, least square method is used and the structure is recalculated using Fourier transforms. (Clark, 2022)

Multi-Component Solids

A multicomponent crystal is a crystal whose basis is made up of multiple components. Crystalline multicomponent solids can be classified according to the simplified flow-scheme below. (Christer B. Aakeröy, 2018)

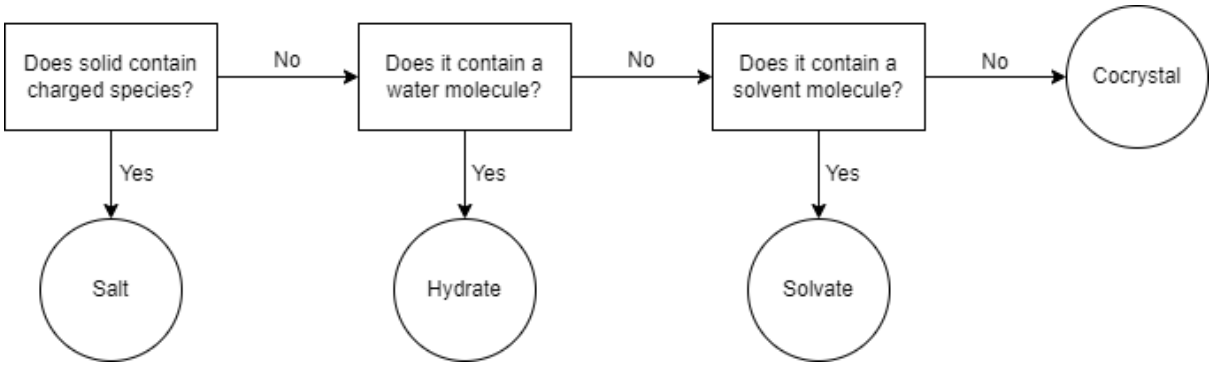

Figure 2: Classification of crystalline multi-component solids. Picture adapted from schematic in "Co-crystals: Preparation, Characterization and Applications" (Christer B. Aakeröy, 2018)

According to (Karimi-Jafari, 2018) the definition of cocrystals is: "solids that are neutral crystalline single phase materials composed of two or more different molecular and/or ionic compounds generally in a stoichiometric ratio which are neither solvates nor simple salts." If at least one of the coformers in a cocrystal is an API and the other is pharmaceutically acceptable, the cocrystal is classified as a pharmaceutical cocrystal. A cocrystal has a crystal structure different to either of the starting materials, resulting in different physiochemical properties. Thus a cocrystal may have superior physicochemical properties compared to either of the pure starting compounds.

Polymorphism and Activation Energy

Polymorphism is when a solid compound exists in different crystalline forms. Polymorphs are chemically identical, but have different forms depending on intermolecular arrangements (polymorphism, 2009). The different crystal structures of polymorphs result in different physiochemical properties (Zhou Y, 2018) and because of the different crystal structures they also have different activation energies. The rate constant of a reaction can be described by Arrhenius equation $k = Ae^{-E_a/RT}$, where k is the reaction rate, E_a is the activation energy, R is the gas constant and T is the temperature in Kelvin. This means that different methods of cocrystallization may result in different polymorphs, as the energy available to the molecules is different for each method. Each polymorph has a different activation energy and Gibbs energy. The concepts of Gibbs energy and activation energy are illustrated in figure 3 below.

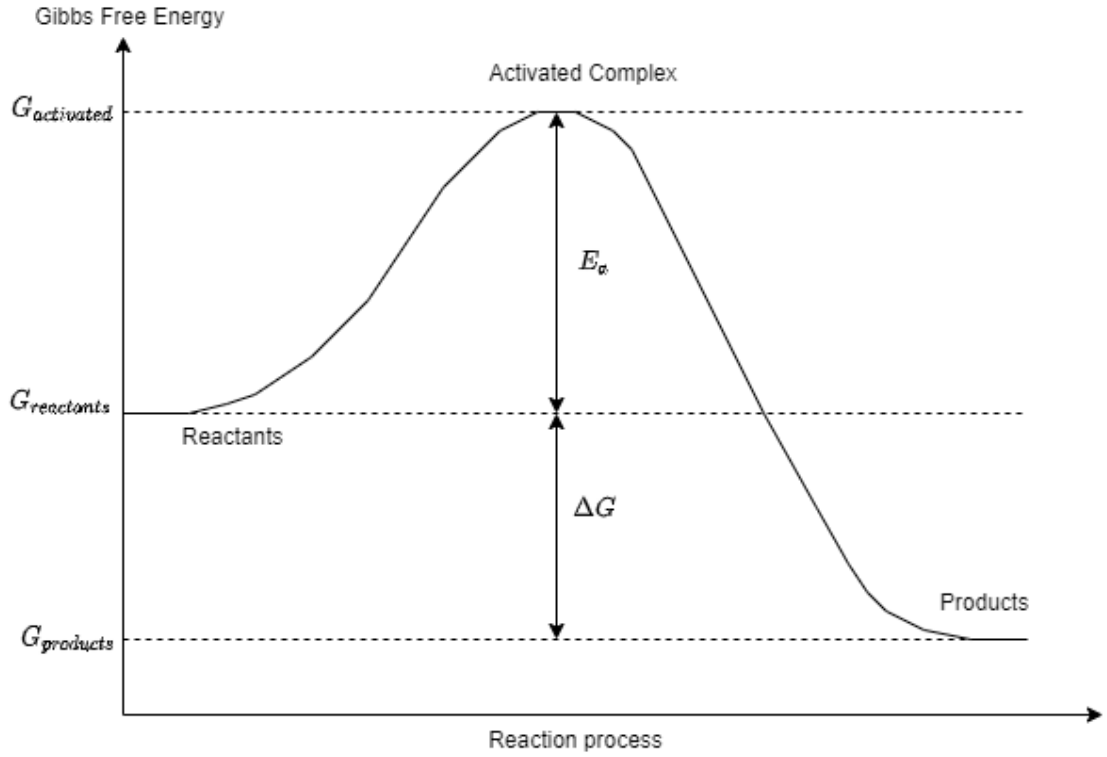

Figure 3: Image illustrating the role of Gibbs free energy and activation energy for a reaction process. ΔG is Gibbs energy for the products subtracted by Gibbs energy for the reactants. Only if $\Delta G < 0$ will the product be stable, as Gibbs energy is minimized at equilibrium. E_a is the activation energy, which is the minimum energy that the reactants needs for the reaction process.

Chemical Equilibrium

According to "An Introduction to Thermal Physics" (Schroeder, 2000), the equilibrium state of a system in room temperature and 1 atm is determined so that Gibbs free energy is minimized. This means that for a chemical reaction at room temperature and 1 atm

$$A + B \leftrightarrow AB,$$

the concentration of each species at equilibrium is determined so that Gibbs free energy is minimized. Gibbs free energy is given by

$$G = U + P \cdot V - T \cdot S,$$

where U is internal energy of the sample, P is pressure, V is volume, T is temperature and S is entropy. For a multicomponent crystal to be stable Gibbs free energy needs to be lower for the multicomponent crystal than the total Gibbs energy for each species on its own. (Schroeder, 2000) Boltzmann distribution/Gibbs distribution gives the probability that a system will be in a specific state as a function of the state's energy and the temperature. The probability of the system being in state i at temperature T, when there are M accessible states to the system is (Schroeder, 2000):

$$p_i = \frac{e^{-\varepsilon_i/k_B T}}{\sum_{j=1}^{M} e^{-\varepsilon_j/k_B T}}$$

This means that the ratio of probability between two states 1 and 2 in a system with an unknown number M of accessible states is given by

$$\frac{p_2}{p_1} = \frac{e^{-\varepsilon_2/k_b T} / \sum_{j=1}^{M} e^{-\varepsilon_j/k_b T}}{e^{-\varepsilon_1/k_b T} / \sum_{j=1}^{M} e^{-\varepsilon_j/k_b T}} = \frac{e^{-\varepsilon_2/k_b T}}{e^{-\varepsilon_1/k_b T}} = e^{-(\varepsilon_2-\varepsilon_1)/k_b T} = e^{-\Delta\varepsilon/k_b T}$$

Here $\Delta\varepsilon = \varepsilon_2 - \varepsilon_1$ is the difference in energy between state 2 and state 1. Note that this equation means that $p_2 > p_1$ only if $\Delta\varepsilon < 0$, that is if state 2 has lower enthalpy than state 1. A larger

negative value of $\Delta\varepsilon$ means a larger value of p_2/p_1. Note that this do not take activation energies into account.

COSMOtherm

COSMOtherm is a COSMO-RS application that can determine the likelihood of a cocrystal forming. COSMO-RS is based on quantum mechanics and thermodynamics, not experimental data. In COSMO-RS the surface charge density of a molecule in a solution is computed with quantum mechanics. (Loschen, 2013) This is simplified by having the surface of the molecule divided into different segments, where each segment has the surface charge density computed. When the surface charge density of two molecules is known, statistical physics can be used determine the energy change when two segments are in contact with each other. The energy change is $E_{m,n}$ between segments m and n, where the surface charge densities are σ_m and σ_n. COSMO-RS takes electrostatic effects, hydrogen bonds, van der Waals interaction and a combinatorial/entropy term into account. Between two segments the energy change is a sum of the following effects (Biovia, 2020)

$$E_{m,n}(electrostatic) \sim (\sigma_m + \sigma_n)^2$$
$$E_{m,n}(Hydrogen\ bonds) \sim \sigma_m \times \sigma_n$$
$$E_{m,n}(van\ der\ Waals) \sim area$$
$$E_{m,n}\ (combinatorial, entropy)$$

In a solution there are many possible contacts between different segments. By looking at the energy change at interaction, the enthalpy difference between molecule A and B interacting with each other and molecule A and B only interacting within themselves can be computed. This is the excess enthalpy for a mixture of compound A and compound B. In this report this computation will be done for two APIs combined with various coformers respectively. The excess enthalpy for an API and a coformer is given by (Loschen, 2013)

$$H_{ex} = H_{API,coformer} - mH_{pure,API} - nH_{pure,coformer},$$

where m:n is the stoichiometric ratio of API to coformer in the mixture. Compounds pairs with $H_{ex}<0$ prefer interacting with each other, over interacting within themselves, as the reaction resulting in the least energy is the most probable interaction. Larger negative H_{ex} corresponds to an increased probability of forming cocrystals. (Loschen, 2013)

Cocrystal Preparation Methods

The cocrystallization methods used in this project are the solid state method of liquid assisted grinding (LAG) and the solution based methods of isothermal slurry conversion and evaporative cocrystallization. LAG involves adding a small amount of solvent, which has a catalytic role in cocrystal formation, prior to grinding. Enough solvent should be added that it persists throughout the grinding process. (Karimi-Jafari, 2018)

Isothermal slurry conversion involves suspension of the target molecule and the coformer in a solvent, such that the solid fraction remains in excess. It does not require full dissolution, resulting in a clear solution, of the target molecule and the coformer. (Karimi-Jafari, 2018)

Evaporative cocrystalization is employed for generating single crystal cocrystals. The method includes the nucleation and growth of a cocrystal from a solution of both the target molecule and the coformer in a solvent. Through enabling evaporation, solvent is removed leading to supersaturation. The supersaturation leads to nucleation and growth of the cocrystal. A slow rate of evaporation ensures formation of a smaller number of larger crystals, while a faster rate leads to a higher number of smaller crystals. A slower rate is usually preferable, (Karimi-Jafari, 2018) as the ideal size of single crystals for SCXRD is the relatively large 150-250µm. (Dutrow, 2022)

Single crystals should be retrieved from the solution before the solvent completely evaporates, to avoid degradation of the crystal and ensure retrieval of a clean crystal. SCXRD is a method for identifying the crystal structure of a single crystal. Identification of the crystal structure is needed to find out if an obtained crystal is a cocrystal, salt, hydrate, or a polymorphic form of the API or coformer. It is ideal to perform evaporative cocrystallization from three solution, one where the API and coformer is in 1:1 stoichiometric ratio, one where the API is in excess and one where the coformer is in excess. This increases the probability of obtaining a cocrystal, along with identifying cocrystals with unequal stoichiometries. One issue with evaporative cocrystallization is that evaporation can be very slow, with evaporation times of up to 6 months being reported. The evaporation time of course depends on the volatility of the solvent. (Karimi-Jafari, 2018)

Method

The method of the thesis was to computationally screen for coformers to form cocrystals with the APIs indapamide and trifluoperazine respectively, and use the results of the computational screening as a basis for experimental screenings. The combinations of APIs and coformers which were likely forming cocrystals according to the experimental screening, were used in attempts to create single crystals through evaporative cocrystallization. Single crystals formed were analyzed with SCXRD. In cases of SCXRD showing the formation of a cocrystal, or a new multicomponent crystal, an attempt was made to recreate the material in powder form for characterization. The two APIs were also characterized, using the methods of PXRD, TGA, DSC and DVS. The different techniques are described in more detail in the method subsections below.

Characterize APIs

Trifluoperazine 2HCl and indapamide were characterized through PXRD (Powder X-Ray Diffraction), TGA (ThermoGravimetric Analysis), DSC (Differential Scanning Calorimetry) and DVS (Dynamic Vapor Sorption). The exact structure was readily found through looking at previous measurements of crystal structure through SCXRD in the Cambridge Structural Database (CSD), a sublet software from the Cambridge Crystallographic Data Centre (CCDC).

PXRD was performed using a Rigaku Miniflex 600 X-ray diffractometer. The results were saved and analyzed with the software SmartLab Studio II. The PXRD measurements were done in reflection mode and the diffraction pattern of the powder collected at a range of $2\theta = 3°: 0.01°: 50°$. The measurement speed was set to 3°/min. Spinning speed was set to 80 rpm and a Cu *K*α source, 40 kV, 15 mA was used as a source for the X-ray beam. (AstraZeneca, 2022)

TGA monitored the weight change that occured as samples of the APIs were heated at a constant rate. It was used to determine thermal stability and presence of any volatile components, such as water molecules. (Dabing Chen, 2009). TGA was performed with the instrument TGA Q500, controlled by the software TA Instruments Explorer. First a platinum cradle with an aluminium cap (without sample inside) was placed in one of the instrument's sample holders and a calibration was performed to set the balance to zero. Then the cradle and the cap were removed and approximately 5 mg of the sample added to the aluminium cap. The cap with sample was placed into the platinum cradle and moved back into the same sample holder that had been calibrated. The settings in the software were set to heat the sample from room temperature to 350ºC, at 5-10ºC per minute, and resulted in a graph showing mass depending on temperature. The decomposition temperature can be read from this graph. (Norberg, 2020) The temperature where weight loss due to decomposition has just started in TGA, was used as the upper limit in DSC measurements.

DSC measured the heat flow into or from samples of the APIs at different temperatures and was performed using the instrument DSC Discovery 2500. This enabled measuring the heat flows associated with transitions in the material as a function of temperature and time. (TA Instruments, 2022) Approximately 2-3 mg of the sample was weighted into an aluminium pan. The samples are heated from -20°C to the upper limit retrieved from TGA, with a heating rate of 3°C/min under a nitrogen purge of 100 mL/min. An empty aluminium pan was used as a reference for DSC. For the measurements closed pans, though not hermetically sealed, were used. The measurements were performed in modulated mode with modulation temperature amplitude set to 1°C and modulation period set to 60 s.

DVS was performed using a Dynamic Vapor Sorption Resolution instrument. A sample of 5-15 mg was pre-sieved and then placed on a microbalance in a controlled atmosphere with room temperature, where it was purged with humid nitrogen. The humidity was changed stepwise at

10% steps from 40% RH to 90% RH, down to 0% RH, and then to 90% RH and back down to 0% RH. A 10% step was taken when the weight change was less than 0.002% during an equilibration time set to a minimum of 30 min, and a maximum of 6 hours. This resulted in an isotherm showing increase of weight due to absorption of vapor from the atmosphere, depending on humidity level. This isotherm is a measure of hygroscopicity. (Vasudha Murikipudi, 2013)

Computational Screen for Cocrystals

There was a computational screen for cocrystals of indapamide and trifluoperazine, provided by the software COSMOtherm. COSMOtherm first determined the surface charge density of the APIs. It used statistical physics of interacting molecular surface segments to compute the excess enthalpy for a mixture of API and coformer compared to pure coformer and pure API. (Loschen, 2013) The step of computing excess enthalpy H_{ex} was done for all combinations of the two APIs with coformers in AstraZeneca's internal database, which are mostly coformers from the GRAS (Generally Recognized As Safe) list and the EAFUS (Everything Added to Food in the US) list. This was done for 1:1, 1:2 and 2:1 stoichiometries. Then Excel was used to rank all combinations on excess enthalpy. The experimental cocrystal screenings were prioritized in order of lowest excess enthalpy to higher. The results of the computational screen can be seen in "Results: Computational Screen for Cocrystals".

Experimental Cocrystal Screening of Trifluoperazine

An attempt was made to experimentally create the theoretically viable cocrystals. This was initially done through combining the APIs with theoretically viable coformers through liquid assisted grinding (LAG) in a planetary ball mill. Heptane, methanol and acetonitrile respectively were used as solvents; 10 µl of solvent was used for each 10 mg of API and coformer. These solvents were chosen as methanol is a polar solvent, heptane is a non-polar solvent and acetone is able to dissolve both polar and non-polar substances, and solution formation has a catalytic role in cocrystallization. For each combination of API, coformer and solvent, 10 mg total of API and coformer were put in a vial. One stainless steel ball of diameter 3 mm diameter was put in the vial. Right before LAG by planetary ball milling 10 µl of the solvent was added in the vial. Twenty-four of these vials, with caps on, were put in the planetary ball mill. The settings for the planetary ball mill were set to 700 rpm for 30 min. After planetary ball milling, the contents of the vials were characterized with PXRD. The coformers were also characterized by PXRD, for comparison. The diffraction patterns of the API, coformer and potential cocrystal were used to determine if a physical mixture of API and coformer had been created, or if a cocrystal had possibly been achieved. (AstraZeneca, 2022)

LAG by mortar and pestle is repeated for the 1:1 stoichiometry of the most promising combinations, using meOH as solvent. For the most promising combinations, meOH is also used as solvent for isothermal slurry conversion. Isothermal slurry conversion is performed for a minimum of 24 hours, using a magnetic stirrer for mixing the slurry. There was an extension of the cocrystal screening, by using liquid assisted grinding by mortar and pestle. Note that PXRD are run on all samples afterwards, for comparison with API and coformer.

There was an attempt to use salts as coformers for cocrystal screening. This attempt was for cases of theoretically viable coformers having a salt form where the cation could theoretically bind to the chloride anion in trifluoperazine 2HCl. The relevant cases are

$$TFP \cdot 2\,HCl + 2\,(K \cdot Acesulfame) \longrightarrow TFP \cdot 2\,Acesulfame + 2\,KCl$$

$$TFP \cdot 2\,HCl + 2\,(Na \cdot Saccharin) \longrightarrow TFP \cdot 2\,Saccharin + 2\,NaCl$$

In these cases isothermal slurry conversion of coformer and trifluoperazine 2HCl in a stoichiometry of 2:1, using the solvents methanol and ethanol respectively, were performed. After at least 24 hours of isothermal slurry conversion, vials of the samples were put in a

centrifugal filter to separate out precipitated material from the slurry. The clear solution above the packed material in the bottom of the vial, was removed, filtered with 0.45 μm filters and transferred into a new vial. The remaining material at the bottom of the original vial was dried and analyzed by PXRD, to confirm that the removed material is KCl and NaCl respectively. In that case, an attempt of growing single crystals through slow evaporating of the corresponding clear solution was made. There was also an attempt to directly grow single crystals through slow evaporation for mixtures at 2:1 stoichiometries of coformer salts and trifluoperazine 2HCl, using the binary solvents MeOH/H_2O and EtOH/H_2O respectively. The binary solvents were mixed in the ratio 1:1 by volume.

Experimental Cocrystal Screening of Indapamide

Experimental cocrystal screening for indapamide, was performed using isothermal slurry conversion for 100 mg of 1:1 stoichiometries of API and coformers. The coformers used were the ones suggested by the computation cocrystal screening through COSMOtherm. Initially the PXRD results of the potential cocrystals were compared only to pure indapamide and pure coformer respectively. The comparison method was later amended to also comparing with the PXRD patterns of Indapamide which had been in isothermal slurry conversion with ACN, and with MeOH.

Creating More Material of Potential Cocrystals

In the cases of potential coformers to trifluoperazine 2HCl which were deemed viable by experimental cocrystal screening, 700 mg mixtures of coformers and APIs in molar stoichiometries of 1:1 were prepared with isothermal slurry conversion. The coformers used for this were etidronic acid monohydrate, oxalic acid and gallic acid. This was not done for the cases of coformer salts, as adequate amounts had already been prepared.

In the cases of potential cocrystals including indapamide which were deemed viable by experimental screening, 500 mg mixtures of coformer and API were prepared with isothermal slurry conversion. The relevant coformers for this were 4,4-bipyridine, 1,10-phenanthroline, 1,5-naphthalenedisulfonic acid tetrahydrate and oxalic acid. The solvents used for this were initially MeOH, but later ACN.

Growing Single Crystals

To grow single crystals of the prospective cocrystals, powder of each potential cocrystal was mixed in different vials with an array of solvents. If the powder formed lumps in the solvent an ultrasonic bath was used to break up the lumps. If all lumps were broken up, but not all powder dissolved into the solution, more solvent was added. The goal was to get transparent, or at least somewhat transparent, solutions. The solution was then filtered. Filtering was done through attaching a hollow needle to a syringe and sucking up the solution, replacing the needle with a filter of pore size 0.45 μm and pressing the solution through the filter into a new vial. This resulted in completely clear, though sometimes slightly colored, solutions. A cap was placed on each vial and depending on the evaporation rate of each solvent, a different number of needles was stuck through the cap to allow evaporation. The solutions were then left to evaporate and checked upon weekly. A microscope was used to identify when single crystals had formed in a solution.

The array of solvents used for growing single crystals, was expanded to include binary solvents for indapamide. This was an attempt to find more cocrystals and multicomponent crystals. The binary solvent of methanol/heptane was suggested by my supervisor. Other binary solvents were decided upon making a short list of common polar solvents used for growing single crystals and a short list of common non-polar solvents. Combinations that were miscible were mixed to be used as binary solvents.

Methanol	Miscible	Not miscible
Ethanol	Miscible	Miscible
Acetone	Miscible	Miscible
Acetonitrile	Miscible	Not miscible
Tetrahydrofuran	Miscible	Miscible
Ethyl Acetate	Miscible	Miscible
Methyl Ethyl Ketone	Miscible	Miscible
Polar solvents / **Nonpolar solvents**	Chloroform	Hexane

Table 1: Above are some common polar solvents and non-polar solvents. The table shows if the combinations are miscible or not. Miscible combinations are marked with green while non-miscible combinations are marked with red. Adding together the miscible combinations of solvents resulted in binary solvents, which were used to expand the array of solvents used for growing single crystals.

Single Crystal Structure Analysis and Refinement of IND·4,4-BPD

Whenever single crystals had formed at evaporation, the crystals were analyzed by SCXRD. The SCXRD of a crystal was performed with a XtaLAB Synergy diffractometer, equipped with a HyPix-Arc 100 detector and Oxford Cryosystem. Measurement was performed at 100 K. Data is measured through several scans determined by the program CrysAlisPro which controls the SCXRD as well as collecting and handling the resulting data. Then ShelXT structure solution program determines the structure and space group of the crystal. A more exact description on how **IND·4,4-BPD** is analyzed with SCXRD is given below. Note that all other single crystals were analyzed in a similar way.

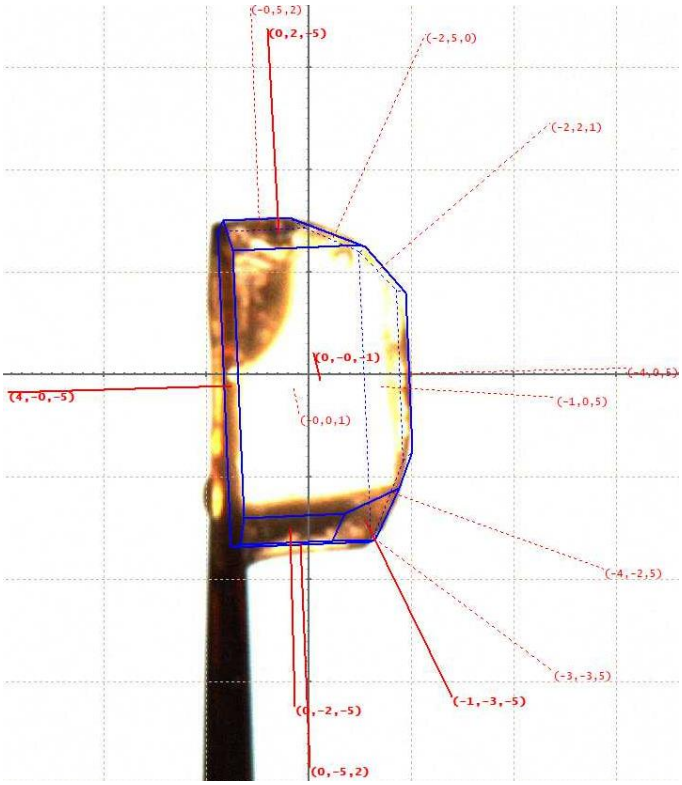

Figure 4: Face indexing of a single crystal of dimensions 0.32 × 0.18 × 0.12 mm³. The single crystal is IND·4,4-BPD

Single clear colourless block-shaped crystals of **IND·4,4-BPD** recrystallised from MeOH by slow evaporation. A crystal, see figure 4 above, with dimensions 0.32 × 0.18 × 0.12 mm^3 was selected and mounted on a MITIGEN holder in perfluoroether oil on the diffractometer. The crystal was kept at a temperature of 100 K during scans with Cu K_α radiation, the number of which were based on the strategy calculation of the program CrysAlisPro. The resulting diffraction patterns were collected and indexed. CrysAlisPro used 26956 reflections, which is equivalent to 58% of the observed reflections, for refining the unit cell. Data reduction, scaling and absorption corrections were also performed using CrysAlisPro. (Rigaku OD, 2022) Numerical absorption correction is based on gaussian integration over a multifaceted crystal model. The face indexing of the analyzed crystal, which can be seen in figure 4 above, was used for this. The crystal structure was solved and the space group determined by the ShelXL (Sheldrick, 2015) structure solution program using dual methods, and refined by full matrix least squares minimisation on $\boldsymbol{F^2}$. All non-hydrogen atoms were refined anisotropically, while most hydrogen atom positions were calculated geometrically and then refined using the riding model. Some hydrogen atoms were refined freely.

Characterization of IND·4,4-BPD

Characterization using TGA, DSC and DVS were done in the same way as described in the "Characterize APIs" section, though this time it is multicomponent crystals instead of APIs that are being characterized. The bulk powder of **IND·4,4-BPD** was prepared by slurrying equimolar amount of indapamide and 4,4-bipyridine in MeOH for more than 24 hours. The resulting slurry was dried using a Smart Evaporator, and subsequently placed in a vacuum chamber. Pure phase of **IND·4,4-BPD** was checked by comparing experimental and simulated PXRD pattern. In the case of **TFP^{2+}·$2Cl^-$·2MeOH** 500 mg of trifluoperazine 2HCl was in isothermal slurry conversion with MeOH for more than 24 hours. The resulting slurry was dried gently using the Smart Evaporator. PXRD was then run on the resulting mix and compared with a simulated PXRD pattern of **TFP^{2+}·$2Cl^-$·2MeOH**.

Results

Characterization of APIs

Characterization of the APIs indapamide and trifluoperazine 2HCl was performed using PXRD, TGA, DSC and DVS as described in "Method: Characterize APIs". The results of this are displayed in the subsections below.

PXRD

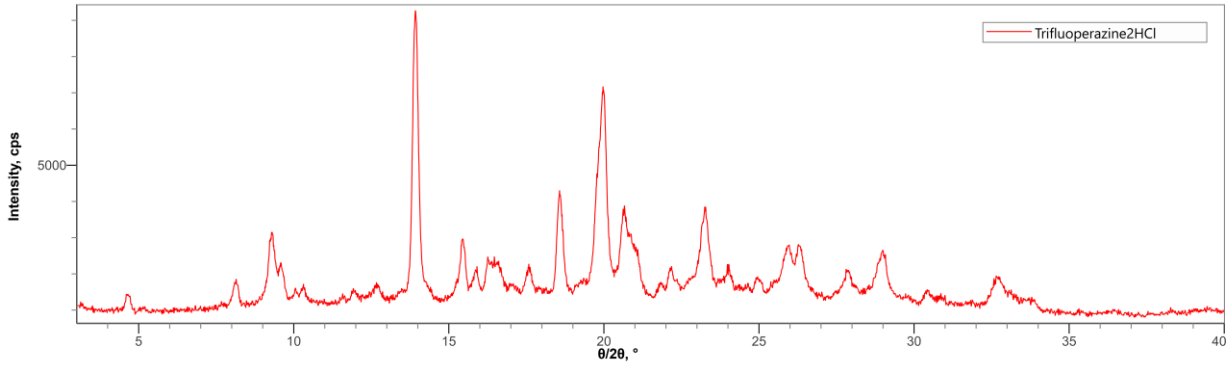

Figure 5: This is the experimentally measured PXRD pattern of trifluoperazine 2HCl.

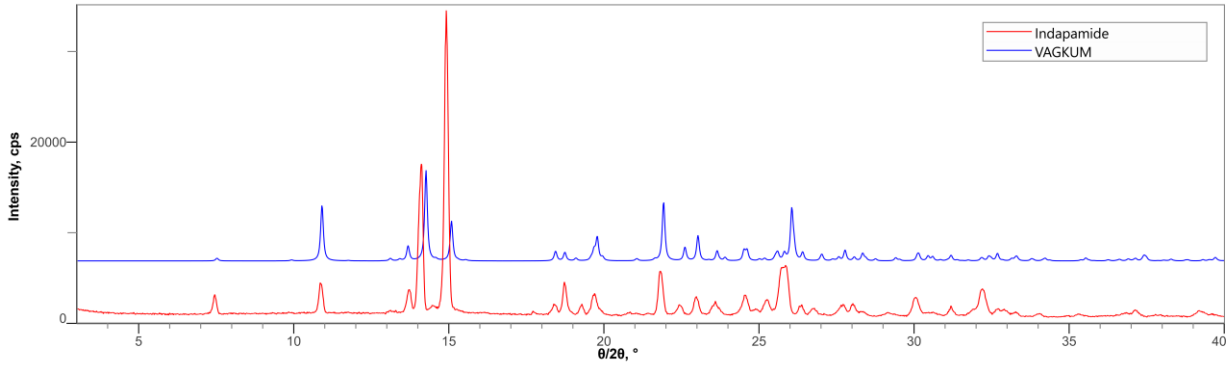

Figure 6: The red line is the experimentally measured PXRD pattern of indapamide. Here the pattern is compared to the PXRD pattern of indapamide hydrate (blue line) computed from the crystal structure of indapamide hydrate (named VAGKUM) from the CSD. This shows that indapamide is hygroscopic with hydrate formation.

TGA and DSC

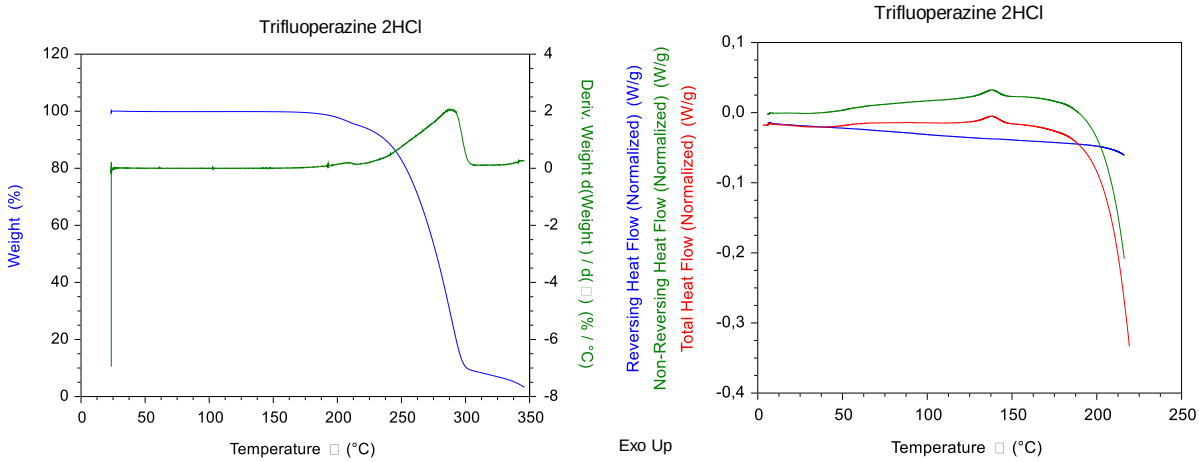

Figure 7: This is the result of thermogravimetric analysis (TGA) and differential scanning calorimetry (DSC) for trifluoperazine 2HCl. The TGA results shows that trifluoperazine 2HCl is thermally stable. Using a weight loss of 2% due to decomposition as the definition for decomposition temperature, the decomposition temperature for trifluoperazine 2HCl is 198℃ *. Regarding the DSC results, the non-reversing heat flow is due to reactions, evaporation or decomposition. The non-reversing heat flow into the sample increases at the temperature where decomposition start.*

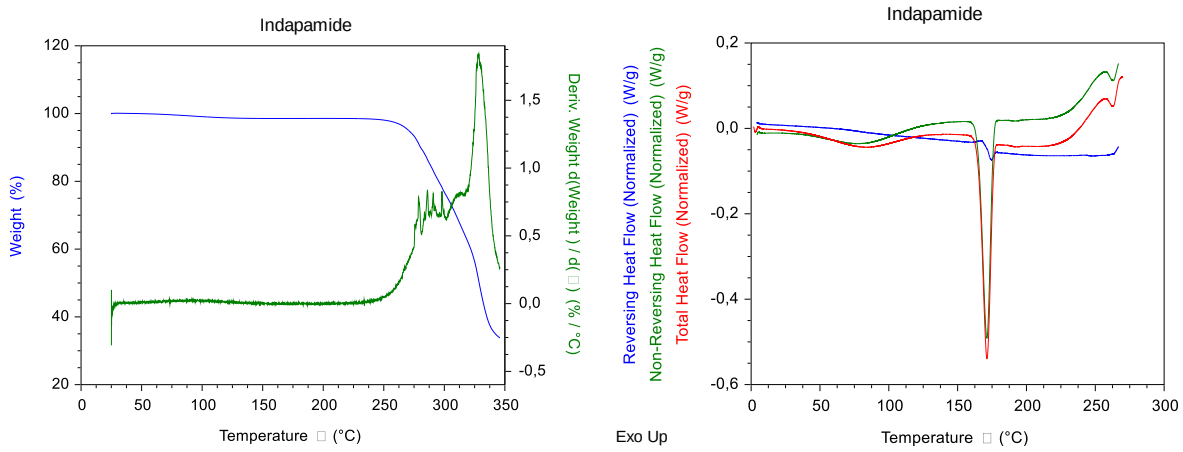

Figure 8: This is the result of thermogravimetric analysis (TGA) and differential scanning calorimetry (DSC) for Indapamide. The TGA results shows that indapamide is thermally stable, though likely has a small amount of water molecules bound to it which are initially evaporating. Using a weight loss of 2% due to decomposition as the definition for decomposition temperature, the decomposition temperature for indapamide is 263℃ *. Regarding the DSC results, there is a melting peak at about* 170℃

DVS

The DVS plot in figure 9 and 10 shows that trifluoperazine 2HCl is very hygroscopic, while indapamide is slightly hygroscopic. The DVS plot of Indapamide also indicate the formation of a stable hydrate.

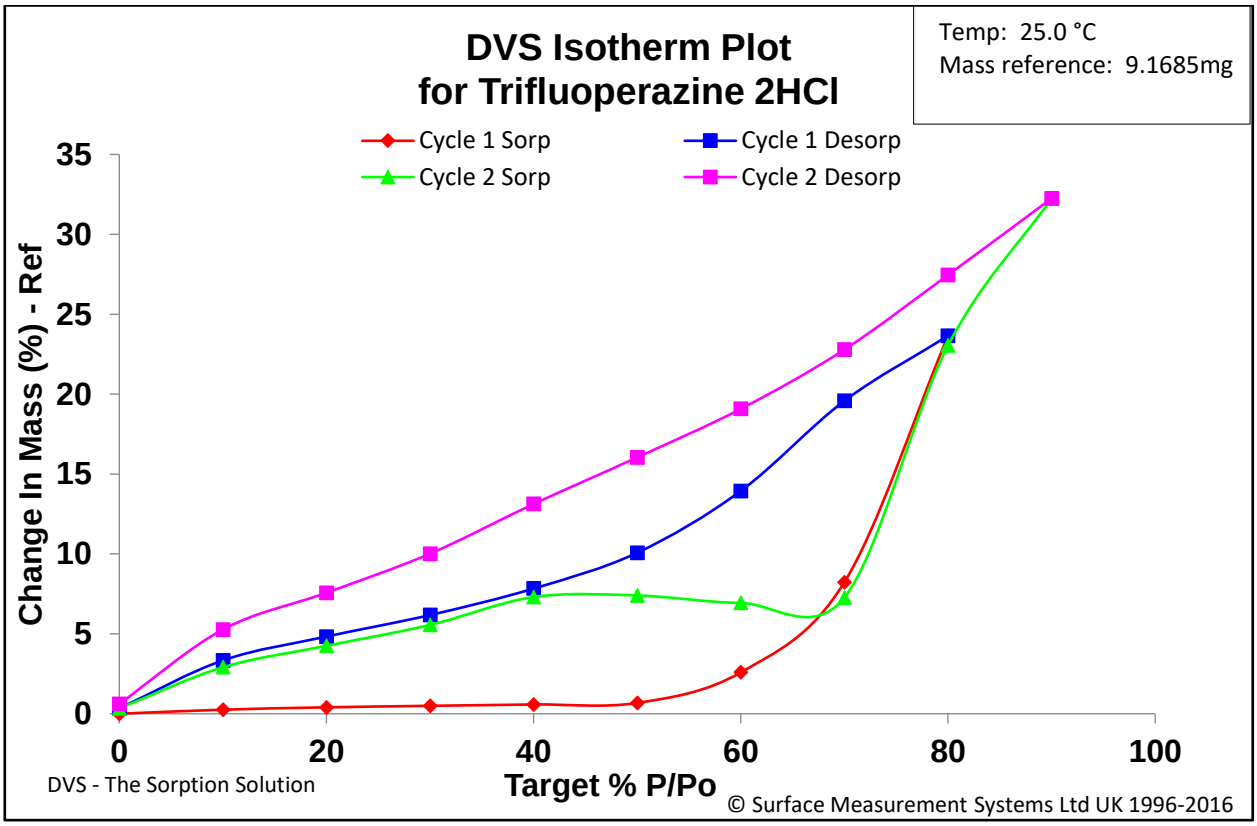

Figure 9: This is a dynamic vapor sorption (DVS) isotherm plot for trifluoperazine 2HCl. The graph shows how the mass change depending on the relative humidity P/P_0, as the relative humidity (RH) changes stepwise with 10% steps in two cycles. The first cycle includes sorption from 0% RH to 80% RH and desorption from 80% RH to 0% RH. The second cycle includes sorption from 0% RH to 90% RH, and desorption from 90% RH to 0% RH. It is clear that trifluoperazine 2HCl is very hygroscopic.

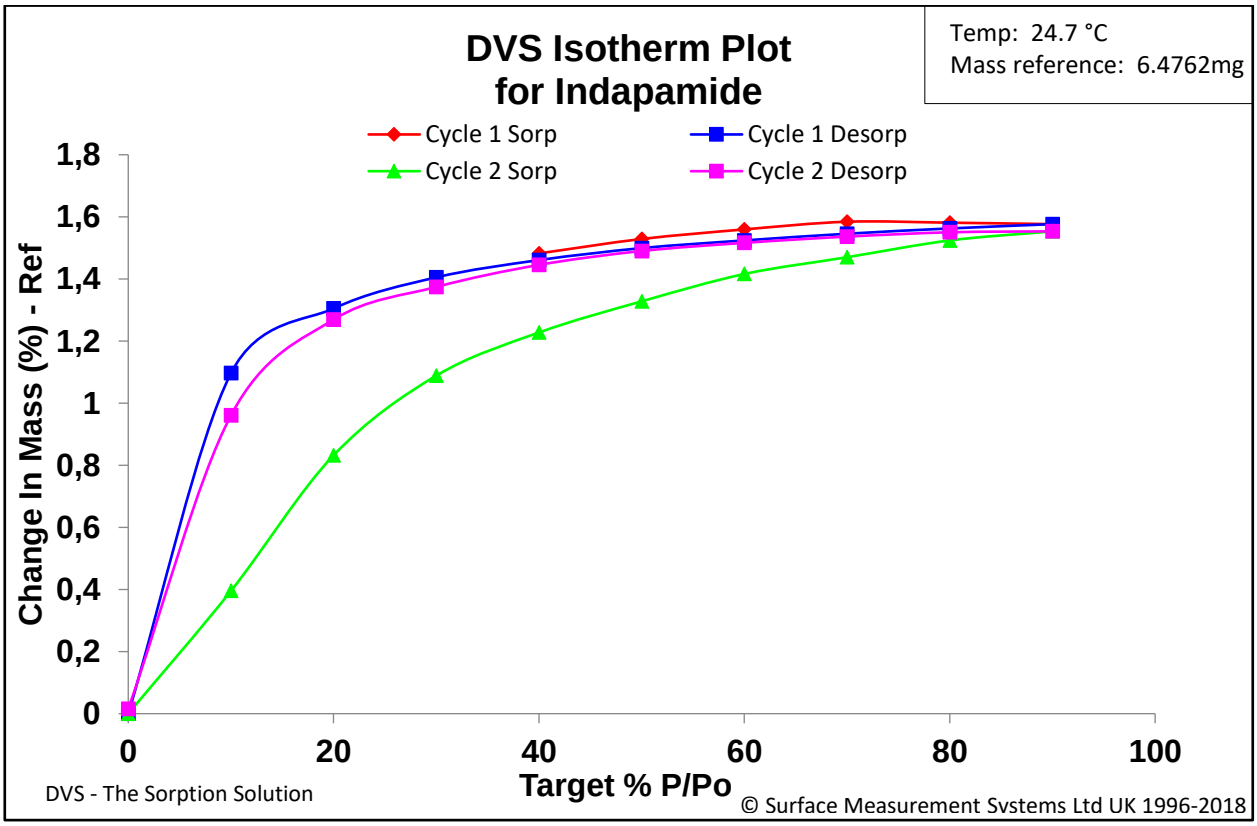

Figure 10: This is a dynamic vapor sorption (DVS) isotherm plot for indapamide. The graph shows how the mass change depending on the relative humidity P/P_0, as the relative humidity (RH) changes stepwise with 10% steps in two cycles. The first cycle includes sorption from 40% RH to 90% RH and desorption from 90% RH to 0% RH. The second cycle includes sorption from 0% RH to 90% RH, and desorption from 90% RH to 0% RH. Indapamide is slightly hygroscopic.

Computational Screen for Cocrystals

Below the results of the computational screen for cocrystals using COSMOtherm are tabulated. The combinations that were experimentally screened are marked with √.

Coformer (Coformer:API)	H_{ex} [kcal/mol]	Molecular mass [g/mol]	Mass coformer [mg] (10 mg total)	Mass API [mg] (10 mg total)	Screened
1,5-Naphthalenedisulfonic acid tetrahydrate (1:1)	-3,88	360,36	4,29	5,71	√
Oxalic acid (1:1)	-3,76	90,3	1,58	8,42	√
Trimesic acid (1:2)	-3,56	210,14	1,79	8,21	√
Pamoic acid (1:1)	-3,53	388,37	4,47	5,53	√
Etidronic acid monohydrate (1:1)	-3,41	224,04	3,18	6,82	√
Trimesic acid (1:1)	-3,39	210,14	3,04	6,96	√
Sulfamic acid (1:1)	-3,36	97,09	1,68	8,32	√
Oxalic acid (1:2)	-3,28	90,3	0,86	9,14	√
1,5-Naphthalenedisulfonic acid tetrahydrate (1:2)	-3,22	360,36	2,73	7,27	√
Sulfamic acid (1:2)	-3,17	97,09	0,92	9,08	√
Isocitric acid (1:2)	-3,16	192,124	1,67	8,33	
Pamoic acid (1:2)	-3,07	388,37	2,88	7,12	√
L-Toluoyl Tartaric acid (1:1)	-3,05	386,35	4,46	5,54	
Fumaric acid (1:1)	-3,04	116,07	1,95	8,05	√
3,5-dihydroxybenzoic acid (1:2)	-3,02	154,12	1,38	8,62	√
Isocitric acid (1:1)	-2,99	192,124	2,86	7,14	
Etidronic acid monohydrate(1:2)	-2,98	224,04	1,89	8,11	√
2,4-dihydroxybenzoic acid (1:1)	-2,95	154,12	2,43	7,57	
Gallic acid (1:1)	-2,93	170,12	2,62	7,38	√
3,5-dihydroxybenzoic acid (1:1)	-2,88	154,12	2,43	7,57	√
Gallic acid (1:2)	-2,88	170,12	1,5	8,5	√
1,5-Naphthalenedisulfonic acid tetrahydrate (2:1)	-2,82	360,36	6	4	√
3,4-Dihydroxybenzoic acid (1:1)	-2,81	154,12	2,43	7,57	
Oxalic acid (2:1)	-2,79	90,3	2,73	7,27	√
Etidronic acid monohydrate (2:1)	-2,72	224,04	4,83	5,17	√
3,4-Dihydroxybenzoic acid (1:2)	-2,67	154,12	1,38	8,62	
L-Toluoyl Tartaric acid (1:2)	-2,64	386,35	2,87	7,13	
Fumaric acid (1:2)	-2,63	116,07	1,08	8,92	√
Pamoic acid (2:1)	-2,61	388,37	6,18	3,82	√
2,4-Dihydroxybenzoic acid (1:2)	-2,6	154,12	1,38	8,62	
Sulfamic acid (2:1)	-2,54	97,09	2,88	7,12	√
3-Hydroxybenzoic acid (1:1)	-2,53	138,12	2,23	7,77	
6-hydroxy-2-naphthoic acid (1:1)	-2,52	188,18	2,81	7,19	
2,5-dihydroxybenzoic acid (1:1)	-2,52	154,12	2,43	7,57	
Gentisic acid (1:1)	-2,44	154,12	2,43	7,57	
4-Hydroxybenzoic acid (1:1)	-2,44	138,12	2,23	7,77	
5-Chlorosalicylic acid (2:1)	-2,44	172,57	4,18	5,82	
Trimesic acid (2:1)	-2,39	210,14	4,67	5,33	√
5-Chlorosalicylic acid (1:1)	-2,38	172,57	2,64	7,36	
1-Hydroxy-2-naphthoic acid (2:1)	-2,35	188,18	4,39	5,61	
2,4-Dihydroxybenzoic acid (2:1)	-2,35	154,12	3,91	6,09	
L-Toluoyl Tartaric acid (2:1)	-2,32	386,35	6,17	3,83	
2,5-dihydroxybenzoic acid (1:2)	-2,31	154,12	1,38	8,62	
1-Hydroxy-2-naphthoic acid (1:1)	-2,31	188,18	2,81	7,19	
Citric acid (1:1)	-2,31	192,12	2,86	7,14	
3-Hydroxybenzoic acid (1:2)	-2,3	138,12	1,26	8,74	
α-Ketoglutaric acid (1:1)	-2,3	146,1	2,33	7,67	
6-Hydroxy-2-naphthoic acid (1:2)	-2,3	188,18	1,64	8,36	
Fumaric acid (2:1)	-2,3	116,07	3,26	6,74	√
Saccharin (2:1)	-2,29	183,18	4,33	5,67	Tested otherwise
Acesulfame K (2:1)	-2,29	201,24	4,56	5,44	Tested otherwise

Table 2: The result of computationally screening for cocrystals of trifluoperazine, ordered from lowest excess enthalpy H_{ex}. The table also includes molecular mass and the mass of API and coformer respectively that is needed to achieve 10 mg total, for each coformer. The molecular masses were retrieved from Merck. Note that trifluoperazine 2HCl has a molecular mass of 480.42 g/mol. (Merck, 2022)

Coformer (Coformer:API)	H_{ex} [kcal/mol]	Molecular mass [g/mol]	Mass coformer [mg] (100 mg total)	Mass API [mg] (100 mg total)	Screened
Piperazine (1:1)	-2,64	86,14	19,06	80,94	√
4,4-bipyridine (1:1)	-2,3	156,18	29,92	70,08	√
N,N-Dimethylpiperazine (1:1)	-2,11	114,19	23,79	76,21	
DL-Valine (1:1)	-1,66	117,15	24,26	75,74	
2,6-dimethylpyrazine (1:1)	-1,62	108,14	22,82	77,18	
Octadecylamine (1:1)	-1,58	269,51	42,42	57,58	
Pyrazine (1:1)	-1,56	80,09	17,96	82,04	
Isoquinoline (1:1)	-1,41	129,16	26,09	73,91	
Dimethylsulfoxide (1:1)	-1,4	78,13	17,6	82,4	
Carnitine (1:1)	-1,32	197,66	35,08	64,92	
Sulfamic acid (1:1)	-1,28	97,09	20,97	79,03	√
1,10-Phenanthroline (1:1)	-1,21	180,21	33	67	√
2,3,5,6-Tetramethylpyrazine (1:1)	-1,2	136,19	27,13	72,87	
Methyl Nicotinate (1:1)	-1,13	137,14	27,27	72,73	
1-Methyl-2-pyrrolidinone (1:1)	-1,12	99,13	21,32	78,68	
1,5-Naphthalenedisulfonic acid tetrahydrate (1:1)	-1,07	360,36	49,62	50,38	√
N,N-Dimethylacetamide (1:1)	-1,05	87,12	19,23	80,77	
Oxalic acid (1:1)	-1,04	90,3	19,8	80,2	√

Table 3: The result of computationally screening for cocrystals of indapamide, ordered from lowest excess enthalpy H_{ex}. Here only the results for the 1:1 molar stoichiometry is displayed, as it was decided to only use that stoichiometry for experimental screening. The table also includes molecular mass and the mass of API and coformer respectively that is needed to achieve 100 mg total for each coformer. The molecular masses were retrieved from Merck. Also note that indapamide has a molecular mass of 365.83 g/mol. (Merck, 2022)

Results of Experimental Cocrystal Screening for Trifluoperazine 2HCl

Coformer	Stoichiometry (coformer:API)	Solvent: (Mass coformer [mg], Mass API [mg])	Partially new form	Comment
Oxalic acid	(1:1)	Heptane:(1.51, 8.30)		Likely oxidation around steel ball for ACN
		MeOH: (1.54, 8.42)	√	
		ACN: (1.55, 8.39)	√	
	(1:2)	Heptane:(0.93, 9.04)		Likely oxidation around steel ball for ACN
		MeOH: (0.85, 9.00)	√	
		ACN: (0.90, 9.16)	√	
	(2:1)	Heptane:(1.51, 8.30)		Amorphous for meOH. Likely oxidation around steel ball for ACN
		MeOH: (1.54, 8.42)		
		ACN: (1.55, 8.39)	√	
Pamoic acid	(1:1)	Heptane:(4.55, 5.55)		
		MeOH: (4.5, 5.41)		
		ACN: (4.50, 5.59)		
	(1:2)	Heptane:(2.84, 7.07)		
		MeOH: (2.87, 7.29)		
		ACN: (2.93, 7.22)		
	(2:1)	Heptane:(6.19, 3.74)		
		MeOH: (6.22, 3.70)		
		ACN: (6.23, 3.77)		
Gallic acid	(1:1)	Heptane:(2.56, 7.36)		
		MeOH: (2.57, 7.35)	√	
		ACN: (2.58, 7.33)	√	
	(1:2)	Heptane:(1.51, 8.48)		
		MeOH: (1.48, 8.50)	√	
		ACN: (1.54, 8.49)		
1,5-Naphthalene disulfonic acid tetrahydrate	(1:1)	Heptane:(4.31, 5.91)		Likely oxidation around steel ball for ACN. MeOH sample spilled
		MeOH: (4.35, 5.73)		
		ACN: (4.41, 5.77)	√	
	(1:2)	Heptane:(2.80, 7.29)		Likely oxidation around steel ball for MeOH
		MeOH: (2.80, 7.43)	√	
		ACN: (2.64, 7.26)	√	
	(2:1)	Heptane:(5.96, 4.08)		Likely oxidation around steel ball for meOH & ACN
		MeOH: (5.92, 4.14)	√	
		ACN: (5.93, 3.98)	√	
Etidronic acid monohydrate	(1:1)	Heptane:(3.17, 6.88)		
		MeOH: (3.28, 6.99)	√	
		ACN: (3.29, 6.70)		
	(1:2)	Heptane:(1.96, 8.16)		
		MeOH: (1.91, 8.40)	√	
		ACN: (1.94, 8.26)		
	(2:1)	Heptane:(4.92, 5.14)		Turned amorphous for MeOH
		MeOH: (4.77, 5.37)		
		ACN: (4.83, 5.17)		
Sulfamic acid	(1:1)	Heptane:(1.78, 8.44)		Hard to see for MeOH
		MeOH: (1.75, 8.42)		
		ACN: (1.65, 8.27)		
	(1:2)	Heptane:(1.00, 9.21)		Amorphous for MeOH
		MeOH: (0.88, 9.09)		
		ACN: (1.01, 9.37)		

Table 4: The table above shows the result of cocrystal screening using the planetary mill, with 10 µl solvent for each sample. √ is used to denote that a combination of trifluoperazine 2HCl, coformer and solvent after planetary milling have a somewhat different PXRD pattern than an overlap of the PXRD patterns of trifluoperazine 2HCl and its coformer. Thus √ denotes the partial creation of a new crystal form, compared to the crystal forms of the trifluoperazine 2HCl and the coformer. This table shows that partially new forms are created for the coformers of oxalic acid, gallic acid, 1,5-naphthalenedisulfonic acid and etidronic acid monohydrate. However, there seems to be no new crystal forms from using heptane as a solvent. In cases where amorphization is avoided, meOH seems more likely than ACN to assist in formation of partially new forms.

Table 4 above shows the results of an initial experimental screening for cocrystals to Trifluoperazine 2HCl. Figure 11 and 12 below are examples of how comparisons of PXRD patterns were done to achieve the results in table 4 above.

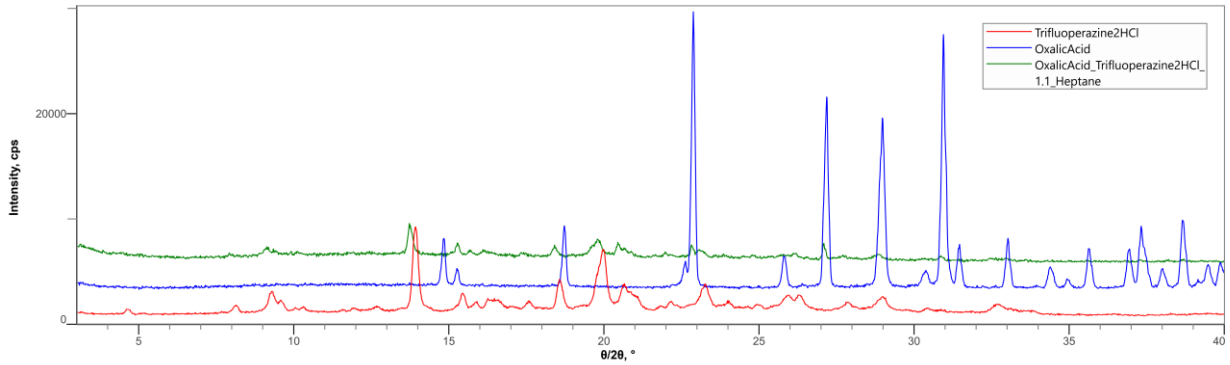

Figure 11: The x-axis (°2ϑ) is the angle between the directions of the incoming X-ray beam and the direction of the diffracted waves. The y-axis shows the intensity in terms of cps (counts per second) for different diffraction angles. The red line shows the PXRD pattern for trifluoperazine 2HCl. The blue line shows the PXRD pattern for oxalic acid. The green line shows the PXRD pattern of oxalic acid and trifluoperazine 2HCl in a molar stoichiometry of 1:1, mixed in a planetary ball mill with heptane as a solvent. The PXRD pattern for oxalic acid mixed with trifluoperazine 2HCl in heptane, looks like an overlap of the PXRD patterns for oxalic acid and trifluoperazine 2HCl respectively. This can be seen by the green line only having peaks which can be seen in either of the other two lines. As described in the "PXRD" theory section, the overlap means that oxalic acid and trifluoperazine 2HCl has been mixed without cocrystallization or reacting in any way.

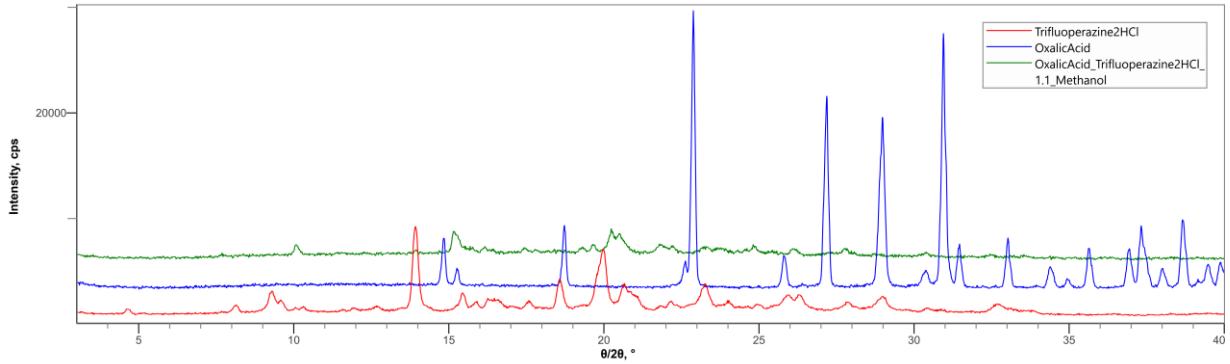

Figure 12: The x-axis (°2ϑ) is the angle between the directions of the incoming X-ray beam and the direction of the diffracted waves. The y-axis shows the intensity in terms of cps (counts per second) for different diffraction angles. The red line shows the PXRD pattern for trifluoperazine 2HCl. The blue line shows the PXRD pattern for oxalic acid. The green line shows the PXRD pattern of oxalic acid and trifluoperazine 2HCl in a molar stoichiometry of 1:1, mixed in a planetary ball mill with methanol as a solvent. The PXRD pattern for oxalic acid mixed with trifluoperazine 2HCl in methanol, looks somewhat different than an overlap of the PXRD patterns for oxalic acid and trifluoperazine 2HCl respectively. This can be seen by the green line having intensity peaks which are not seen in either of the other two lines; which is the case for the two green peaks around $2\theta \approx 20.5^{\circ}$*. It can also be seen by the green line not having a visible peak at an angle with a very strong intensity peak for one of the other two lines. This is the case at angles* $2\theta \approx 23^{\circ}, 27^{\circ}, 29^{\circ}, 31^{\circ}$ *where the blue line has very strong intensity peaks that are not at all visible in the green line. As described in the theory section "PXRD", the change in PXRD pattern means a change in form when oxalic acid and trifluoperazine 2HCl are mixed with methanol in a planetary ball mill.*

From the results in table 4 it seems that MeOH was the most suitable solvent for cocrystal screening. This as MeOH was most likely to assist in the formation of partially new forms. LAG is repeated for the 1:1 combinations of the most promising combinations, using MeOH as solvent. For the most promising combinations, isothermal slurry conversion was attempted using MeOH as solvent. The results can be seen in table 5 below. Isothermal slurry conversion was performed for a minimum of 24 hours.

Coformer (coformer:API)	Mass coformer [mg], Mass API [mg]	Preparation method	New form	Comment
1,5-Naphthalenedisulfonic acid tetrahydrate (1:1)	21.47, 28.45	LAG, ACN then MeOH as solvent	√	New form 1, different form than New form 2
	42.85, 57.25	Slurry in MeOH		Overlay, could be because of vacuum drying
	42.80, 57.17	Slurry in MeOH	√	New form 2, different form than New form 1
Etidronic acid monohydrate (1:1)	15.96, 34.10	LAG with MeOH	*	
	31.83, 68.20	Slurry in MeOH	√	
Gallic acid (1:1)	13.10, 36.92	LAG with MeOH	*	
	26.22, 73.84	Slurry in MeOH	√	
Oxalic acid (1:1)	8.00,42.19	LAG with MeOH	*	
	15.98, 84.15	Slurry in MeOH	√	

*Table 5: The table above shows the results of cocrystal screening with LAG by mortar and pestle, and cocrystal screening by isothermal slurry conversion. √ denotes a new form. * denotes a somewhat new form.*

Figure 13 and figure 14 below are examples of how comparisons of PXRD patterns were performed to achieve the results in table 5 above. Figure 13 shows the screening of oxalic acid:trifluoperazine 2HCl (1:1). The solvent is MeOH and both the results of LAG and isothermal slurry conversion are included. Figure 14 shows the screening of trifluoperazine 2HCl:1,5-naphthalenedisulfonic acid tetrahydrate (1:1).

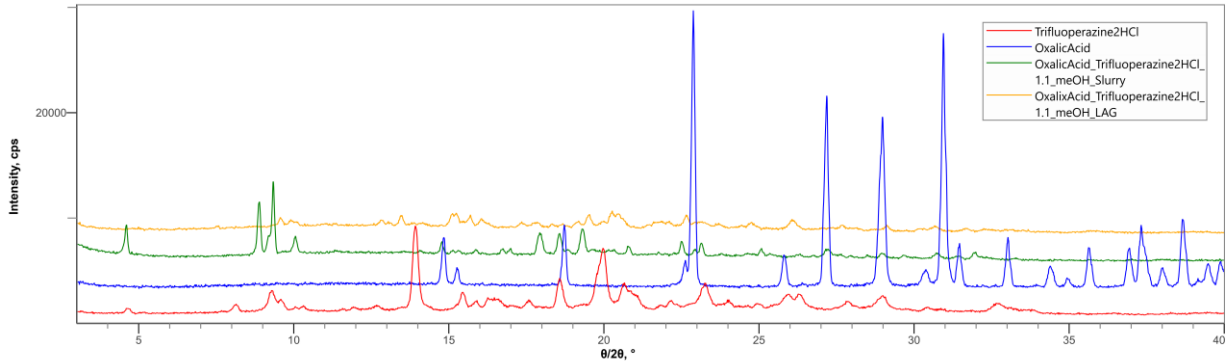

Figure 13: The red line shows the PXRD pattern for trifluoperazine 2HCl (TFP 2HCl). The blue line shows the PXRD pattern for oxalic acid (OA). The green line shows the PXRD pattern for OA and TFP 2HCl mixed in a molar stoichiometry of 1:1 in a MeOH slurry. The yellow line shows the PXRD pattern for OA and TFP 2HCl in a stoichiometry of 1:1 mixed with meOH in LAG. When comparing to the PXRD patterns of OA and TFP 2HCl, it is clear that the combination of OA and TFP 2HCl in isothermal slurry conversion has created a new form whose PXRD pattern is not an overlap of the API and the coformer. This is less clear when LAG is used, in which case it is ambiguous if the PXRD pattern is an overlap or not. The PXRD pattern resulting from LAG mostly look like an overlap with some pattern changes.

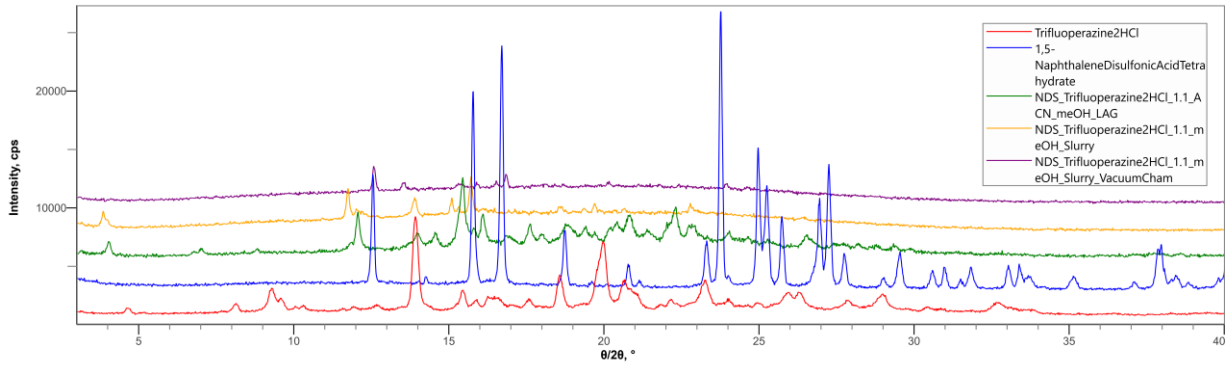

Figure 14: The red line shows the PXRD pattern for trifluoperazine 2HCl (TFP 2HCl). The blue line shows the PXRD pattern for 1,5-napthalenedisulfonic acid tetrahydrate (NDST). The purple and yellow lines show NDST and TFP 2HCl in a stoichiometry of 1:1 mixed in slurry with meOH. The difference is that the purple line is the result of the material being dried in a vacuum chamber. The green line shows NDST and TFP 2HCl in a molar stoichiometry of 1:1 mixed with ACN in LAG, and then MeOH in LAG.

New crystalline forms are created for each of the coformers in table 5. However, the crystal forms are different depending on the method of attempted cocrystallization. This suggests polymorphism. For gallic acid, oxalic acid and etidronic acid monohydrate, very promising results were yielded by isothermal slurry conversion. For 1,5-naphthalenedisulfonic acid tetrahydrate as coformer the result was clearly a new form, but the pattern was not as distinct as for the other combinations. This made gallic acid, oxalic acid and etidronic acid monohydrate the best options as coformers for continued analysis. The results of continued cocrystal screening with new coformers, using LAG, can be seen in table 6 below.

Coformer (coformer:API)	Mass coformer [mg], Mass API [mg]	Preparation method	PXRD Results
Trimesic acid (1:2)	1.95,8.31	LAG, Heptane then ACN	Overlap
Trimesic acid (1:2)	1.94,8.31	LAG, MeOH	Overlap
Trimesic acid (1:1)	3.11,7.08	LAG, Heptane then ACN	Overlap
Trimesic acid (1:1)	3.21,7.10	MeOH	Overlap
Fumaric acid (1:1)	2.02, 8.06	LAG, Heptane, then ACN, then MeOH	Overlap, amorphosity when MeOH is used
Fumaric acid (1:1)	2.05, 8.22	LAG, MeOH	Overlap
Fumaric acid (1:2)	1.23,9.03	LAG, Heptane, then ACN, then MeOH	Overlap
3,5-dihydroxybenzoic acid (1:1)	2.55, 7.75	LAG, Heptane, then ACN	Overlap
3,5-dihydroxybenzoic acid (1:1)	2.58, 7.58	LAG, MeOH	Overlap
3,5-dihydroxybenzoic acid (1:2)	1.57, 8.70	LAG, Heptane, the ACN, then MeOH	Overlap, amorphicity when MeOH is used
3,5-dihydroxybenzoic acid (1:2)	1.41,8.68	LAG, MeOH	Overlap

Table 6: Results of continued cocrystal screening, with new coformers from the computational screen for cocrystals. The API is trifluoperazine 2HCL. The method used is liquid assisted grinding (LAG), and after LAG with a new solvent PXRD is performed on the resulting powder. An example is the case of fumaric acid with trifluoperazine 2HCl in a stoichiometry of 1:1 on the fifth row. First LAG was performed with heptane and the resulting powder characterized with PXRD; the PXRD pattern was clearly an overlap of the PXRD pattern of fumaric acid and the PXRD pattern of trifluoperazine 2HCl. Then LAG was performed with ACN on the same powder and the powder subsequently characterized with PXRD. That PXRD pattern was also an overlap. This was then repeated with MeOH, in which case the PXRD pattern showed amorphicity. On the row below is thus an attempt to repeat that experiment, using only MeOH as a solvent. The resulting PXRD pattern was then an overlap.

Table 7 below shows the results for when the cocrystal screening was altered to include coformer salts. This screening included attempts to grow single crystals, which is also included in the section “Results of Single Crystal Growth”. PXRD of the resulting salts show promising results, but any resulting single crystals are either NaCl, KCl or Acesulfame K. One case of NaCl was ambiguous, as the material analyzed with SCXRD was somewhat amorphous with wide diffraction peaks.

Combination	Mass coformer [mg] Mass API [mg]	Preparation method	Result
Acesulfame K: Trifluoperazine 2HCl (2:1)	380.91 319.26	Slurry in MeOH, separate salt, evaporative cocrystallization	PXRD of salt looks like mostly KCl, crystal formed when growing single crystal is pure Acesulfame K
	380.98 319.30	Slurry in EtOH, separate salt, evaporative cocrystallization	PXRD of salt show almost only KCl, crystal formed at evaporation is likely KCl, due to small volume of lattice base. Filtering out the salt didn't remove all KCl
	381.02 319.17	Dissolve in MeOH/H20 (1:1 v/v), evaporative cocrystallization	After evaporating, the solvents separated into layers
	381.09 319.22	Dissolve in EtOH/H20 (1:1 v/v), evaporative cocrystallization	After evaporating, the solvents separated into layers
Saccharine Na: Trifluoperazine 2HCl (2:1)	323.45 376.87	Slurry in MeOH, separate salt, evaporative cocrystallization	PXRD of salt look like pure NaCl. Crystal formed at evaporating is NaCl. Filtering out the salt did not remove all NaCl
	323.19 376.65	Slurry in EtOH, separate salt, evaporative cocrystallization	PXRD of salt look like only NaCl. Crystal formed at evaporation is likely NaCl The SCXRD peaks were wide.
	323.25 376.81	Dissolve in MeOH/H20 (1:1 v/v), evaporative cocrystallization	After evaporating, the solvents separated into layers
	323.49 376.85	Dissolve in EtOH/H20 (1:1 v/v), evaporative cocrystallization	After evaporating, the solution became unclear.

Table 7: This table shows the results for when cocrystal screening was altered to include coformer salts. This screening was done differently and includes the growing of single crystals. The preparation method and the results are described above. More information on the preparation method are in the "Experimental Cocrystal Screening of Trifluoperazine" section. Information on evaporative cocrystallization is in the "Growing Single Crystals" section. The results of growing single crystals are also displayed in the section "Results of Single Crystal Growth".

Results of Experimental Cocrystal Screening for Indapamide

Table 8 below shows the results of experimental cocrystal screening for indapamide, performed using isothermal slurry conversion for 100 mg of 1:1 molar stoichiometries of API and coformers. Isothermal slurry conversion was used instead of LAG or planetary ball milling, as the PXRD patterns were more distinctive when using isothermal slurry conversion instead of LAG or planetary ball milling for trifluoperazine cocrystal screening. Only the molar stoichiometry of 1:1 was included in these experiments, to cut down the number of experiments needed. This was deemed acceptable as cocrystal screening for trifluoperazine with a planetary mill tended to result in partially new forms for all stoichiometries of a combination of API and coformer, or none of the stoichiometries. The solvents of heptane, ACN and MeOH were initially used, but heptane was later removed as a solvent as it seemed to result in PXRD patterns which were overlaps for all cases. Result 1 is where comparison of PXRD patterns was only performed with pure indapamide and pure coformers. Result 2 is where the PXRD patterns are also compared to indapamide which has gone through isothermal slurry conversion with MeOH and ACN respectively. Comparison of PXRD patterns was otherwise performed in the same way as in "Results of Experimental Cocrystal Screening for Trifluoperazine 2HCl". The results in the table show that 4,4-bipyridine, 1,10-phenanthroline, oxalic acid and 1,5-naphthalenedisulfonic acid are likely to be forming cocrystals with indapamide.

Combination	Solvent	Mass coformer [mg] Mass API [mg]	Result 1	Result 2
Piperazine: Indapamide (1:1)	Heptane	19.01 81.08	Overlap	----------
	ACN	19.05 81.11	New form	Overlap
	MeOH	19.03 80.95	New form	Overlap
4,4-bipyridine: Indapamide (1:1)	Heptane	29.95 70.06	Overlap	----------
	ACN	30.01 70.26	New form	New form, Likely cocrystal
	MeOH	29.96 70.10	New form	New form, Likely cocrystal
1,10-phenanthroline: Indapamide (1:1)	Heptane	32.93 67.01	Unclear	----------
	ACN	32.99 67.18	New form	New form, Likely cocrystal
	MeOH	32.94 67.18	New form	Overlap
Oxalic Acid: Indapamide (1:1)	ACN	19.95 80.33	New form	New form, Likely cocrystal
	MeOH	19.93 80.35	New form	Overlap
1,5-Naphtlenedisulfonic acid tetrahydrate: Indapamide (1:1)	ACN	49.78 50.48	New form	New form, Likely cocrystal
	MeOH	49.63 50.46	New form	Overlap
Sulfamic acid: Indapamide (1:1)	ACN	20.93 79.16	New form	Overlap (possibly due to insolubility)
	MeOH	20.91 79.05	New form	Overlap (possibly due to insolubility)
Tromethamine: Indapamide (1:1)	ACN	25.06 75.32	New form	Overlap
	MeOH	25.00 75.17	New form	Overlap

Table 8: The preparation method used for cocrystal screening is isothermal slurry conversion. Result 1 is when comparison of PXRD patterns is only done with pure indapamide and pure coformers. Result 2 is when the PXRD patterns are also compared to indapamide which has gone through isothermal slurry conversion with MeOH and ACN respectively.

Figure 15 below shows the PXRD patterns for indapamide which has gone through isothermal slurry conversion with ACN, indapamide which has gone through isothermal slurry conversion with MeOH and indapamide that has not gone through isothermal slurry conversion.

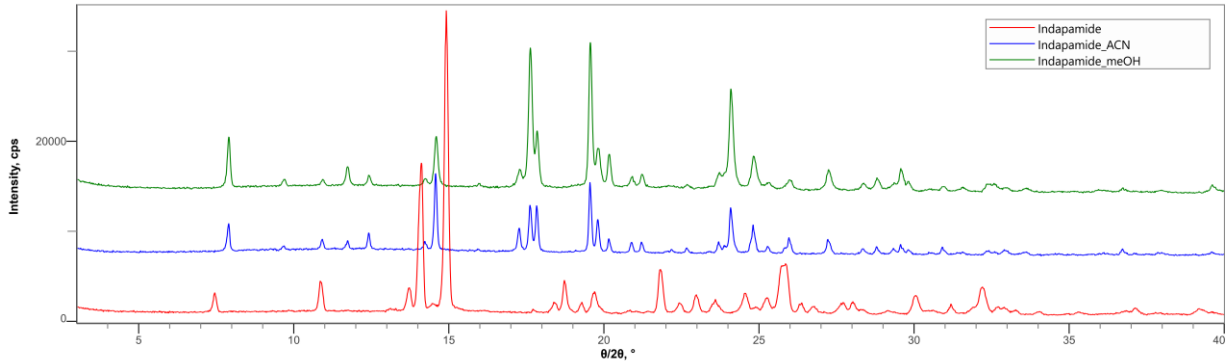

Figure 15: The red line shows the PXRD pattern for indapamide. The blue line shows the PXRD pattern for indapamide which has been in isothermal slurry conversion with ACN. The green line shows the PXRD pattern for indapamide which has been in isothermal slurry conversion with MeOH. The blue and green lines are identical, but different from the red PXRD pattern of indapamide that has not been in isothermal slurry conversion.

Figure 15 above shows that indapamide changes form during isothermal slurry conversion, for both ACN and MeOH. Solvate formation being the reason for the PXRD pattern change is unlikely as the PXRD pattern is the same for isothermal slurry conversion with both MeOH and

ACN. It is possible that isostructural solvates have formed; that is where the crystal structure of the two solvates is the same even though the solvents are different. The formation of isostructural solvates can be ruled out using TGA-MS, that is TGA where the vaporized gas is analyzed with mass-spectrometry. More likely possibilities are that the pattern change is either due to polymorphism or hydrate formation. The new PXRD pattern was compared to the already known PXRD patterns of indapamide in different forms. As indapamide is known to exist as three different forms of hydrates, the PXRD pattern of indapamide in a slurry with MeOH/ACN was compared to the PXRD pattern of indapamide hydrates. It is clear from figure 16 below that the new PXRD pattern is not identical to any of the PXRD patterns of known indapamide hydrates. The new PXRD pattern is thus likely due to polymorphism, unless it is a previously unobserved hydrate form.

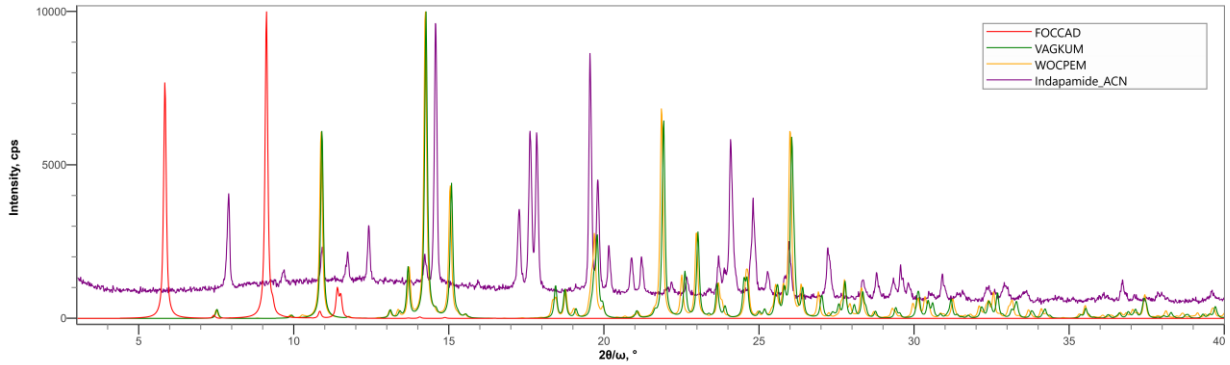

Figure 16: PXRD pattern of indapamide slurried in ACN (which is identical to the pattern for indapamide slurried in meOH) is compared to the PXRD patterns of the indapamide hydrates. The indapamide hydrates are named FOCCAD, VAGKUM and WOCPEM in CSD. It is clear that an indapamide hydrate is not created when indapamide is slurried in ACN. The new pattern is thus likely due to polymorphism.

Results of Single Crystal Growth

The results of attempting to grow single crystals including either trifluoperazine 2HCl or indapamide are shown in table 9, 10 and 11 below. For each attempt of growing a crystal, light grey is used to denote that no crystal has grown yet and dark grey denotes that no crystal has grown despite complete evaporation of solvent. Dark grey can also denote that a crystal is unlikely to grow for some other reason, in which case the reason is specified. If a crystal has formed, that is noted along with the result of analyzing the crystal. In cases where there are two results, it is because a solution formed two different types of crystal or there was an attempt to repeat the experiment because of poor crystal quality.

Solvent	**TFP 2HCl: Oxalic acid (1:1)**	**TFP 2HCl: Etidronic acid monohydrate (1:1)**	**TFP 2HCl: Gallic acid (1:1)**	**TFP 2HCl**
Methanol (3)	New Crystal (TFP^{2+}·2Cl·2MeOH)	Crystal (poor quality)	Became glue	
Ethanol (3)		Lumps produced		
Aceton (1)	Crystal (poor quality)			
ACN (3)	New Crystal, (TFP^{2+}·$2Cl^-$·2ACN)			New Crystal (TFP^{2+}·$2Cl^-$·2ACN)
THF (3)	Crystal (poor quality)			Crystal (poor quality) Crystal (poor quality)
EtOAc (1)		Crystalline, not diffracting	Crystal (poor quality)	Crystal (poor quality)
MEK (3)		Crystal (poor quality)		Crystal (poor quality)
Chloroform (1)				
1,4-dioxane (2)		Pieces produced	Crystalline, not diffracting	----------
Cyclopentyl methyl ether (2)	----------	----------		----------
2-methyl tetrahydrofuran (2)		----------		----------
2-butanol (2)	----------	----------	----------	Pieces produced
DMF (2)	----------	----------	----------	
Toluene (2)	----------	----------	----------	

Table 9: Table with the results from attempted growing of single crystals. For each prospective cocrystal and solvent, or API and solvent, the table lists what was generated. Light grey color denotes that no cocrystal has grown yet and ----- on a white background denotes that this combination was not tried. Dark grey denotes that no crystal has grown, despite complete evaporation, or that the experiment is unlikely to yield a result for some other reason. If another reason, the reason is noted as well. Red color denotes the formation of a crystal, which has too low quality or is too fragile for SCXRD. Green color denotes the formation of a crystal relevant for the thesis. These experiments resulted in the new crystals TFP^{2+}·$2Cl^-$·2MeOH and TFP^{2+}·$2Cl^-$·2ACN, which were both previously unknown. However, only the structure of TFP^{2+}·$2Cl^-$·2MeOH could be fully resolved.

Solvent	**Acesulfame K:TFP 2HCl (2:1)**	**Na Saccharin:TFP 2HCl (2:1)**
Methanol (3)	Crystal (Acefulfame K)	Crystal (NaCl)
Ethanol (3)	Crystal (KCl)	Crystal (NaCl or crystalline in glass phase)
MeOH/H20 (2)	Solution separated into layers	Solution separated into layers
EtOH/H20 (2)	Solution separated into layers	Solution became unclear

Table 10: Table with the results from attempted growing of single crystals, from the attempt of using coformer salts instead of coformers. More information about this attempt can be found in table 7. The color dark grey denotes that the solution is unlikely to yield a result. The reason is listed if it is something else than no crystal formation despite complete evaporation. The color blue denotes the formation of a single crystal which could be analyzed with SCXRD, but which is not relevant for the thesis.

In the cases of "Crystal (poor quality)" it is possible that the experiment can be repeated and the structure resolved, but it was not possible with the SCXRD diffractometer that was used at the time. It was later discovered that the SCXRD diffractometer at Chalmers is better at resolving poor quality crystals than the one used at AstraZeneca. The combinations labelled poor quality could thus be repeated, and potentially resolved using a higher quality SCXRD diffractometer.

Solvent (# needles)	**4,4-Bipyridine: Indapamide (1:1)**	**1,10-Phenanthroline: Indapamide (1:1)**	**Oxalic Acid: Indapamide (1:1)**	**1,5-Naphtlenedisulfonic acid tetrahydrate: Indapamide (1:1)**
Methanol (3)	Crystal (IND·4,4-BPD)			Crystal (pure NDS) Crystal (NDS, NH_4)
Ethanol (3)	Crystal (IND·4,4-BPD)		Crystal (poor quality) Crystal (oxalic acid metal complex with etOH and H_2O)	Crystal (pure NDS) Crystal (NDS solvate)
Aceton (1)	Crystal (poor quality)			Crystal (poor quality) Crystal (poor quality)
ACN (3)	Crystal (IND·4,4-BPD)			Crystal (pure NDS), Crystal (NDS, H_2O, ACN complex)
THF (3)				
EtOAc (1)				Crystal (too fragile)
MEK (3)			Possible contamination	Crystal (poor quality), Crystal (resolved)
Chloroform (1)				
4:1 meOH:Heptane (2)	Pieces produces			Pieces produced
3:1 meOH:Chloroform (2)	----------	Pieces produced	Pieces produced	Pieces produced
1:1 etOH:Chloroform (2)	----------		Crystal (sodium hydrogen oxalate monohydrate)	Pieces produced
1:1 Acetone:Chloroform (1)	----------	Became glue	Crystal (oxalic acid hydrate)	Crystal (NDS, ACN)
1:1 ACN:Chloroform (2)	----------	Crystalline, don't diffract	Crystal (resolved)	Crystal (NDS hydrate)
1:1 THF:Chloroform (2)	----------	Became glue	Crystal (oxalic acid hydrate)	Crystal (NDS hydrate)
1:1 EtOAc:Chloroform (1)	----------		Crystal (sodium hydrogen oxalate monohydrate)	
1:1 MEK:Chloroform (2)	----------	Became glue		
1:1 etOH:Hexane (2)	----------	Became glue	Pieces produced	Pieces formed, not crystals
1:1 Acetone:Hexane (1)	----------		Crystal (sodium hydrogen oxalate monohydrate)	Crystal (NDS with disordered solvent) New Crystal (NDS, N-isopropyl-2-methyl-indolin-1-amine, H_2O)
1:1 THF:Hexane (2)	----------		Crystal (oxalic acid)	
1:1 EtOAc:Hexane (1)	----------	Crystalline, not diffracting	Crystal (boron, oxalic acid complex)	
1:1 MEK:Hexane (2)	----------			Crystal (couldn't resolve)

Table 11: Table with results from attempted growing of single crystals. For each prospective cocrystal and solvent, the table lists what was generated. The color light grey denotes that no crystal has grown yet and ----- on a white background denotes that a combination wasn't tried. Dark grey denotes that no crystal has grown, despite complete evaporation, or that the solution is unlikely to yield single crystals for some other reason. In that case, the reason is listed. Red denotes the formation of a crystal, with too poor quality to be analyzed with SCXRD or that the structure could not be identified with SCXRD. Blue color denotes the formation of a single crystal identified with SCXRD which is not relevant for the thesis. Green color denotes the formation of a crystal relevant for the thesis. The experiments resulted in finding the cocrystal IND·BPD and discovering a previously unknown cocrystal hydrate including 1,5-naphtalenedisulfonic acid (NDS) and N-isopropyl-2-methyl-indolin-1-amine (IMIA). The molecule N-isopropyl-2-methyl-indolin-1-amine is previously unknown.

The most noteworthy result is the discovery of the trifluoperazine salt solvate of **TFP^{2+}·2Cl^-·2MeOH** and the discovery of the cocrystal hydrate **IMIA·2NDS·2H_2O**, where IMIA is an abbreviation given to the previously unknown molecule **N-isopropyl-2-methyl-indolin-1-amine**. These are structures which are not in CSD. Note that **N-isopropyl-2-methyl-indolin-1-amine** is the result of decomposition of indapamide. The cocrystal **IND·4,4-BPD** was also found. Other single crystals were either of too poor quality for analysis, or already known and not including the API. One exception is the trifluoperazine salt solvate TFP^{2+}·2Cl^-·2ACN, whose exact structure could not be resolved.

Due to complete evaporation leading to deterioration of some combinations which yielded single crystals, those experiments were repeated to achieve better crystal quality. When analyzing single crystals, some unexpected results were found. Growing crystals of indapamide and 1,5-naphthalenedisulfonic acid tetrahydrate in meOH resulted in a crystal of 1,5-naphthalenedisulfonic acid and ammonia. This is unexpected as the previous result of this combination was pure 1,5-naphthalenedisulfonic acid crystals, and ammonia was not included in the solution to start with. Ammonia must either be the result of a reaction, or the result of contamination. The crystal with NDS and NH_4 is previously known, but the structure was resolved with higher accuracy than that of previous attempts at resolving the structure available in the CSD. The result of a Na oxalic acid complex after slow evaporation of oxalic acid and indapamide in acetone/hexane binary solvent was unexpected, as neither of the materials used should contain sodium. The result of a boron oxalic acid complex after slow evaporation of oxalic acid in EtOAc/hexane binary solvent was also unexpected, as no materials including boron were used in any of the experiments. The most probable explanation is some kind of contamination.

TFP^{2+}·2Cl^-·2MeOH

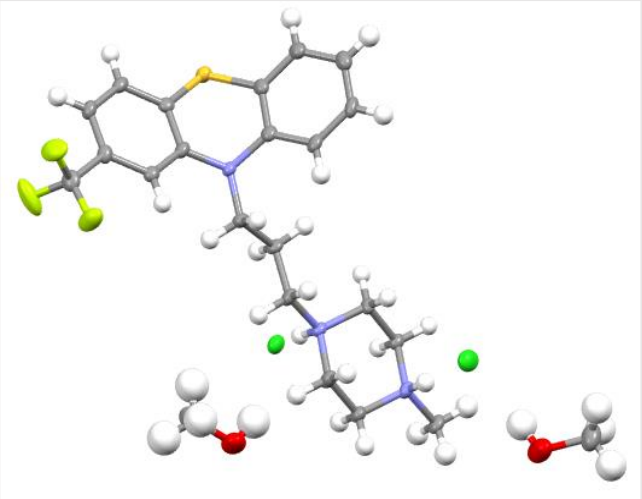

Figure 17: Molecular structure of the trifluoperazine salt solvate TFP^{2+}·2Cl^-·2MeOH.

The molecular formula for **TFP^{2+}·2Cl^-·2MeOH** is $C_{23}H_{34}Cl_2F_3N_3O_2S$ with the formula weight $M_r = 544.49\ g/mol$. The structure is simple orthorombic with the space group $P2_12_12$. The conventional unit cell has lengths a = 7.1480 Å, b = 37.2866 Å, c = 9.8093 Å with angles $\alpha = \beta = \gamma = 90°$. The conventional unit cell has volume V = 2614.42 $Å^3$. There is a single molecule in the asymmetric unit, which is represented by the reported sum formula. However, four sets of TFP^{2+}·2Cl^-·2MeOH fits inside the conventional unit cell. In other words: Z is 4 and Z' is 1. The final wR2 was 0.1313 (all data) and R1 was 0.0523. Crystal data on the structure are tabulated in table 12 below.

Crystal Data

Formula	$C_{23}H_{34}Cl_2F_3N_3O_2S$	*a* [Å]	7.1480
$D_{calc.}$ [g cm^{-3}]	1.383	*b* [Å]	37.2866
μ/mm^{-1}	3.391	*c* [Å]	9.8093
Formula Weight [amu]	544.49	α	90°
Colour	clear colourless	β	90°
Shape	needle-shaped	γ	90°
Size [mm^3]	----------	V [$Å^3$]	2614.42
Crystal System	simple orthorombic	*Z*	4
Space Group	$P2_12_12_1$	*Z'*	1

Table 12: Data on the crystal and its crystal structure. Note that the unit cell dimensions concern the conventional unit cell, which contains 4 sets of TFP^{2+}·2Cl^-·2MeOH

PXRD

The figure below displays PXRD pattern of **TFP^{2+}·$2Cl^-$·2MeOH** as computed by Mercury and compares it to the PXRD pattern of the powder resulting from isothermal slurry conversion of trifluoperazine 2HCl with MeOH. It is clear that the structure of **TFP^{2+}·$2Cl^-$·2MeOH** was not achieved in powder form, as the PXRD patterns are different.

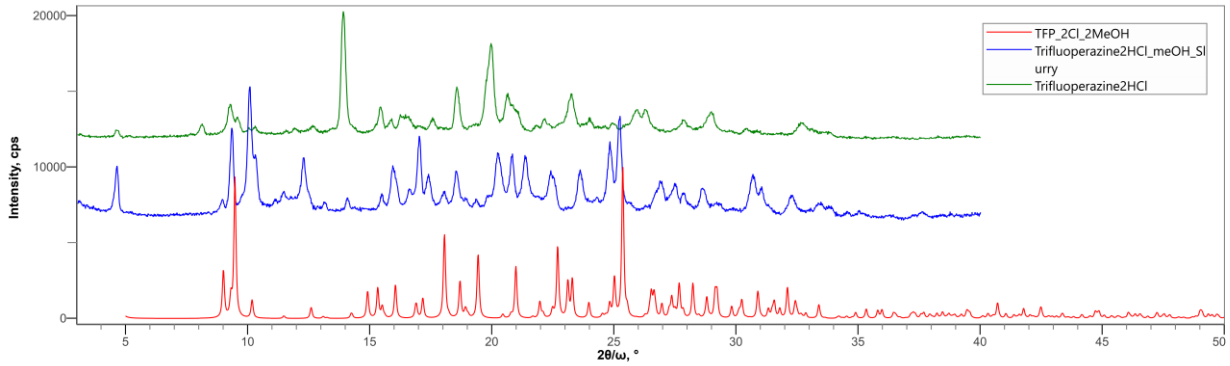

Figure 18: The red line is the PXRD pattern of TFP^{2+}·$2Cl^-$·2MeOH as computed by Mercury from the structure of a single crystal analyzed through SCXRD. The green line is the experimentally measured PXRD pattern, from the powder resulting from isothermal slurry conversion of trifluoperazine 2HCl with meOH. The blue line shows the experimentally measured PXRD pattern of untreated trifluoperazine 2HCl. The three PXRD patterns are all different. It is clear that the same structure was not achieved from isothermal slurry conversion of trifluoperazine 2HCl with MeOH, as when growing the single crystal TFP^{2+}·$2Cl^-$·2MeOH. Characterization of the powder achieved through isothermal slurry conversion will thus not apply to material from which the trifluoperazine salt solvate crystal structure was obtained.

IMIA·2NDS·2H_2O

The molecular formula for the crystal **IMIA·2NDS·2H_2O** is $C_{22}H_{27}N_2O_8S_2$ with the formula weight $M_r = 511.57 g/mol$. The structure is monoclinic with the space group $P2_1/c$. The conventional unit cell has lengths a = 12.106Å, b = 9.831Å, c = 20.601Å with angles $\alpha = \gamma = 90°$ and $\beta = 97.106°$. The conventional unit cell has volume $V = 2432.88$ Å^3 . There is a single molecule in the asymmetric unit, which is represented by the reported sum formula. However, four sets of the **IMIA·2NDS·2H_2O** fits inside the conventional unit cell. In other words: Z is 4 and Z' is 1. The final wR_2 was 0.1070 (all data) and R_1 was 0.0382. The molecular structure is shown in figure 19 below and crystal data on the structure are tabulated in table 13 below. Note that the crystal structure is note completely refined, and some small changes can be expected.

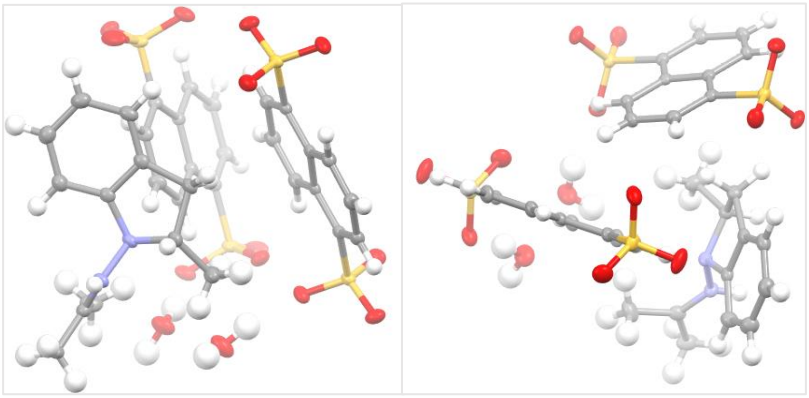

Figure 19: Molecular structure of the cocrystal hydrate IMIA·2NDS·2H_2O. The structure is seen from two different directions.

Crystal Data

Formula	$C_{22}H_{27}N_2O_8S_2$	*A* [Å]	12.106
$D_{calc.}$ [g cm^{-3}]	1.397	*B* [Å]	9.831
μ [mm^{-1}]	2.419	*C* [Å]	20.601
Formula Weight [amu]	511.57	α	90°
Colour	----------	β	97.106°
Shape	block-shaped	γ	90°
Size [mm^3]	----------	V [Å^3]	2432.88
Crystal System	monoclinic	*Z*	4
Space Group	$P2_1/c$	*Z'*	1

Table 13: Data on the crystal and its crystal structure. Note that the unit cell dimensions concern the conventional unit cell, which contain four sets of IMIA·2NDS·2H_2O.

N-isopropyl-2-methyl-indolin-1-amine

The previously unknown molecule **N-isopropyl-2-methyl-indolin-1-amine** (IMIA) was found when growing single crystals. It is one of the molecules in the cocrystal made from decomposed Indapamide and 1,5-Naphthalenedisulfonic acid. The molecules used for growing the single crystal is shown below in table 14, along with the molecules in the single crystal.

Molecules when growing single crystal	Molecules in single crystal
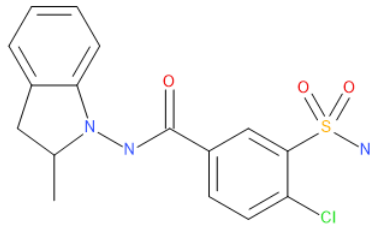 Indapamide	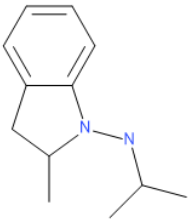 N-isopropyl-2-methyl-indolin-1-amine
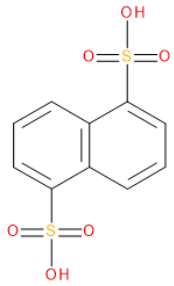 1,5-Naphtalenedisulfonic acid	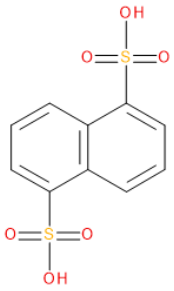 1,5-Naphtalenedisulfonic acid
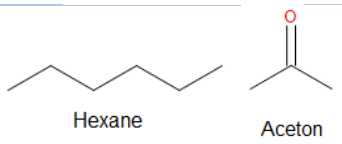 Hexane Aceton	

Table 14: This table shows the molecules used when growing the single crystal and the molecules the single crystal consists of.

It is clear that **N-isopropyl-2-methyl-indolin-1-amine** is a degradation product of indapamide. The decomposition is most likely due to an acid catalysed hydrolysis of the amine bond in indapamide followed by the now liberate amine functionality attacking the electrophile carbonyl carbon in acetone with the subsequent loss of water in an imine condensation. The reaction scheme would then be as described in figure 20 below. (Kennepohl, 2022)

Reaction Step 1	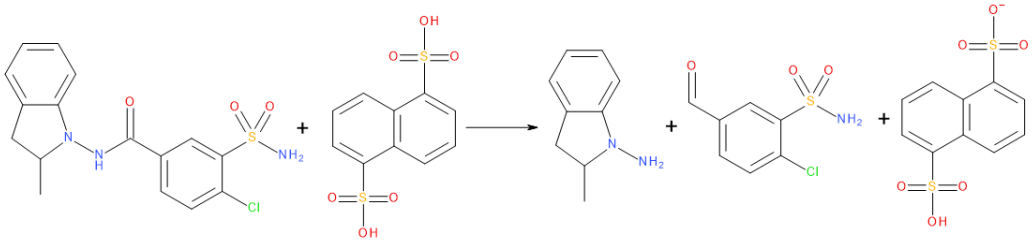
Reaction Step 2	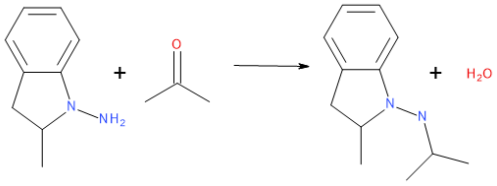

Figure 20: Reaction scheme for indapamide decomposing into N-isopropyl-2-methyl-indolin-1-amine

IND·4,4-BPD

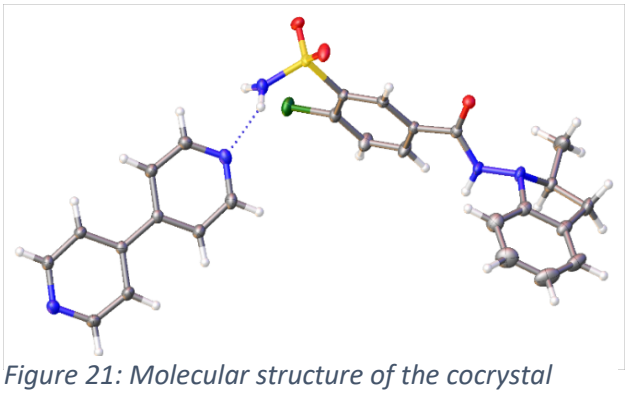

Figure 21: Molecular structure of the cocrystal IND·4,4-BPD

The molecular formula for **IND·4,4-BPD** is $C_{26}H_{24}ClN_5O_3S$ with the formula weight $M_r = 522.01\ g/mol$. The structure is monoclinic with a P21/n head group. The conventional unit cell has lengths a = 7.16094 Å, b = 9.01001 Å, c = 38.3824 Å with angles β = 95.1631°, α= γ = 90°. The conventional unit cell has volume V = 2466.39 Å^3. There is a single molecule in the asymmetric unit, which is represented by the reported sum formula. However, four sets of **IND·4,4-BPD** fits inside the conventional unit cell. In other words: Z is 4 and Z' is 1. The final wR2 was 0.0933 (all data) and R1 was 0.0342. Crystal data on the structure are tabulated in table 15 below.

Crystal Data

Formula	$C_{26}H_{24}ClN_5O_3S$	a [Å]	7.16094
$D_{calc.}$ [g cm^{-3}]	1.406	b [Å]	9.01001
μ [mm^{-1}]	2.488	c [Å]	38.3824
Formula Weight [amu]	522.01	α	90°
Colour	clear colourless	β	95.1631°
Shape	block-shaped	γ	90°
Size [mm^3]	0.32×0.18×0.12	V [Å^3]	2466.39
Crystal System	monoclinic	Z	4
Space Group	$P2_1/n$	Z'	1

Table 15: Data on the crystal and its crystal structure. Note that the unit cell dimensions concern the conventional unit cell, which contain four sets of IND·4,4-BPD.

PXRD

The figure below shows the PXRD pattern as computed from the crystal structure of **IND·4,4-BPD**, and the PXRD pattern of the powder resulting from indapamide and 4,4-bipyridine (1:1) in isothermal slurry conversion with MeOH. As the PXRD patterns in the figure are identical, it confirms that the resulting powder has the crystal structure of **IND·4,4-BPD**. The powder is used for further characterization in TGA, DSC and DVS.

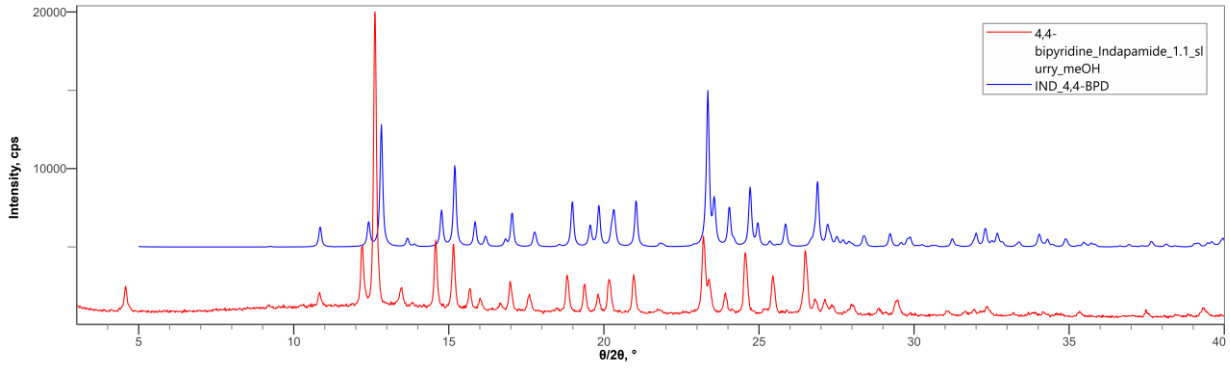

Figure 22: The red line shows the PXRD pattern from indapamide and 4,4-bipyridine (1:1) after isothermal slurry conversion in meOH for at least 24 hours. The blue line shows the PXRD diffractogram of the cocrystal IND·4,4-BPD, as computed from the crystal structure found through SCXRD of a single crystal of the cocrystal. The PXRD patterns are identical, which means that the crystal structure is the same for the powder as for the single crystal. Characterization of the powder from isothermal slurry conversion will thus provide more information on the properties of the material for which the crystal structure was determined.

TGA and DSC

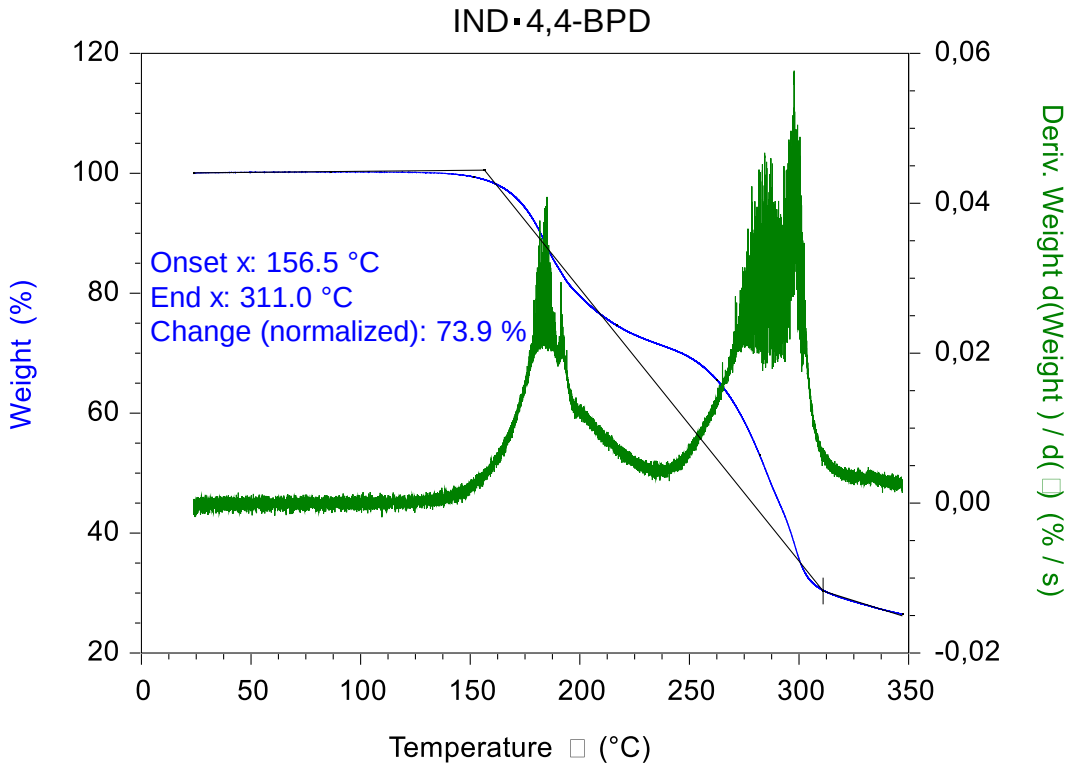

Figure 23: This is the result of thermogravimetric analysis for IND·4,4-BPD. The blue line shows the weight of the sample in % of the initial sample weight. The green line shows the speed of the change in weight, in % per minute. Weight loss for the sample only happens above $156°C$.

Figure 23 above shows that the sample of **IND·4,4-BPD** is anhydrous. This suggests that the material is not very hygroscopic, as a very hygroscopic sample would have absorbed water which would then be removed as temperature increase. There is a massive weight loss starting at approximately $156°C$ due to decomposition. Figure 24 below shows the reversing heat flow, non-reversing heat flow and total heat flow into a sample of **IND·4,4-BPD**. The small peak at $\sim$110℃ is probably due to a small amount of excess coformer that melted, as the literature melting point of 4,4-bipyridine is 111℃. (PubChem, 2022) Using the reversing heat flow, the heat capacity of **IND·4,4-BPD** is calculated by the TA Instruments Trios application to be $0.88J/(g \cdot ℃)$ at 25℃.

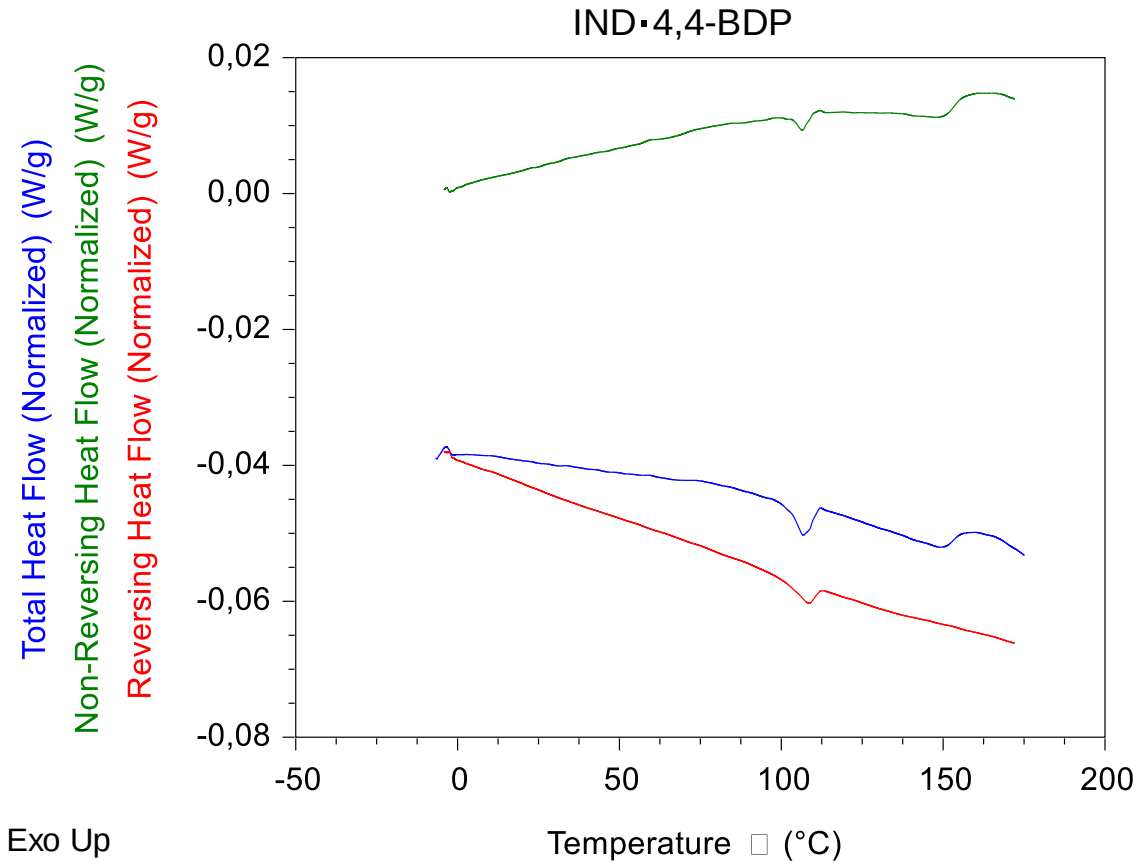

Figure 24: This is the result of differential scanning calorimetry (DSC) for IND·4,4-BPD. The non-reversing heat flow (green) shows the heat flow for evaporation, reactions and decomposition. The reversing heat flow shows the heat flow due to heat capacity, glass transitions and melting. The red graph shows the total heat flow. There is a small peak at ~110℃, which is very close to the literature melting point of 111℃ for 4,4-bipyridine. The peak is probably due to a small amount of excess coformer that melted.

DVS

The API indapamide is slightly hygroscopic, as shown by the indapamide DVS plot in figure 10. In figure 25 and 26 below the DVS plots of the coformer 4,4-bipyridine and the cocrystal **IND·4,4-BPD** are shown. It is clear that 4,4-bipyridine is very hygroscopic with hydrate formation at approximately 40% RH. The hygroscopicity of **IND·4,4-BPD** is considerably lower than the hygroscopicity of the API and much lower than the hygroscopicity of the coformer. As the water uptake of **IND·4,4-BPD** only causes 0.5% increase in mass for 90% RH, the cocrystal is not hygroscopic.

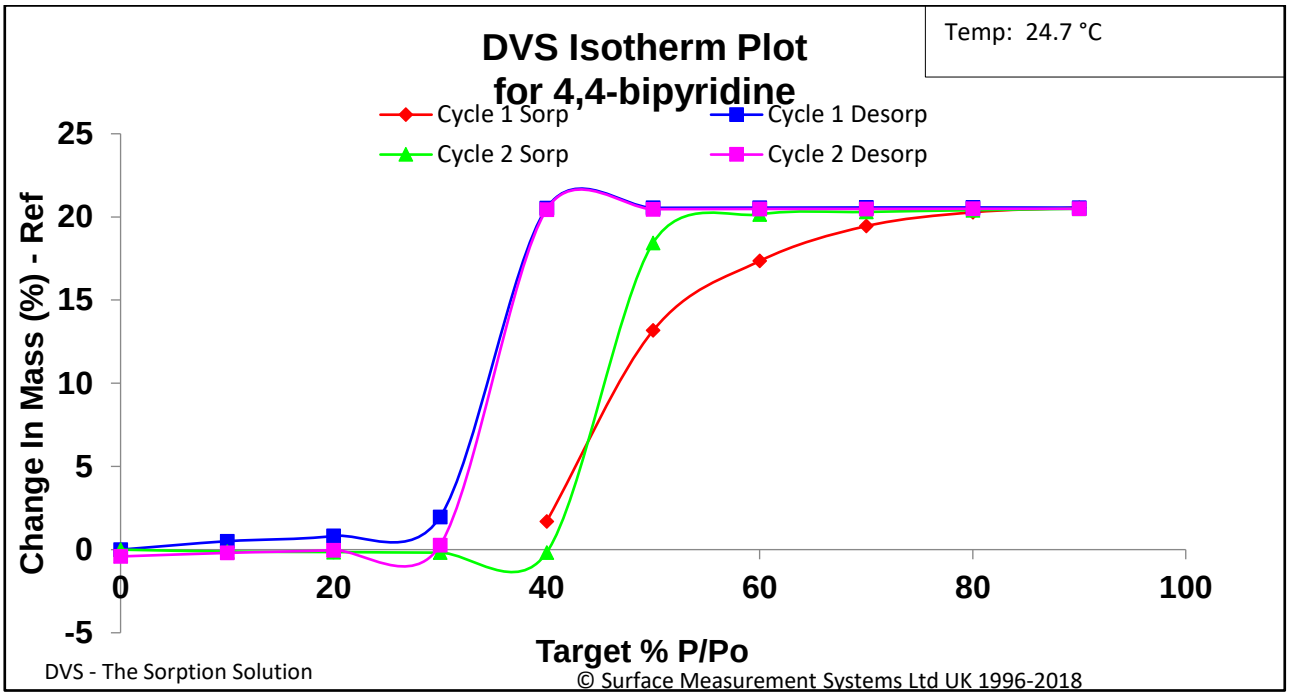

Figure 25: This is a dynamic vapor sorption (DVS) isotherm plot for 4,4-bipyridine. The graph shows how the mass change depending on the relative humidity P/P_0, as the relative humidity (RH) changes stepwise with 10% steps in two cycles. The first cycle includes sorption from 40% RH to 90% RH and desorption from 90% RH to 0% RH. The second cycle includes sorption from 0% RH to 90% RH, and desorption from 90% RH to 0% RH. 4,4-bipyridine is hygroscopic and the hysteresis in the plot indicates that a hydrate is formed at relative humidities above 40%.

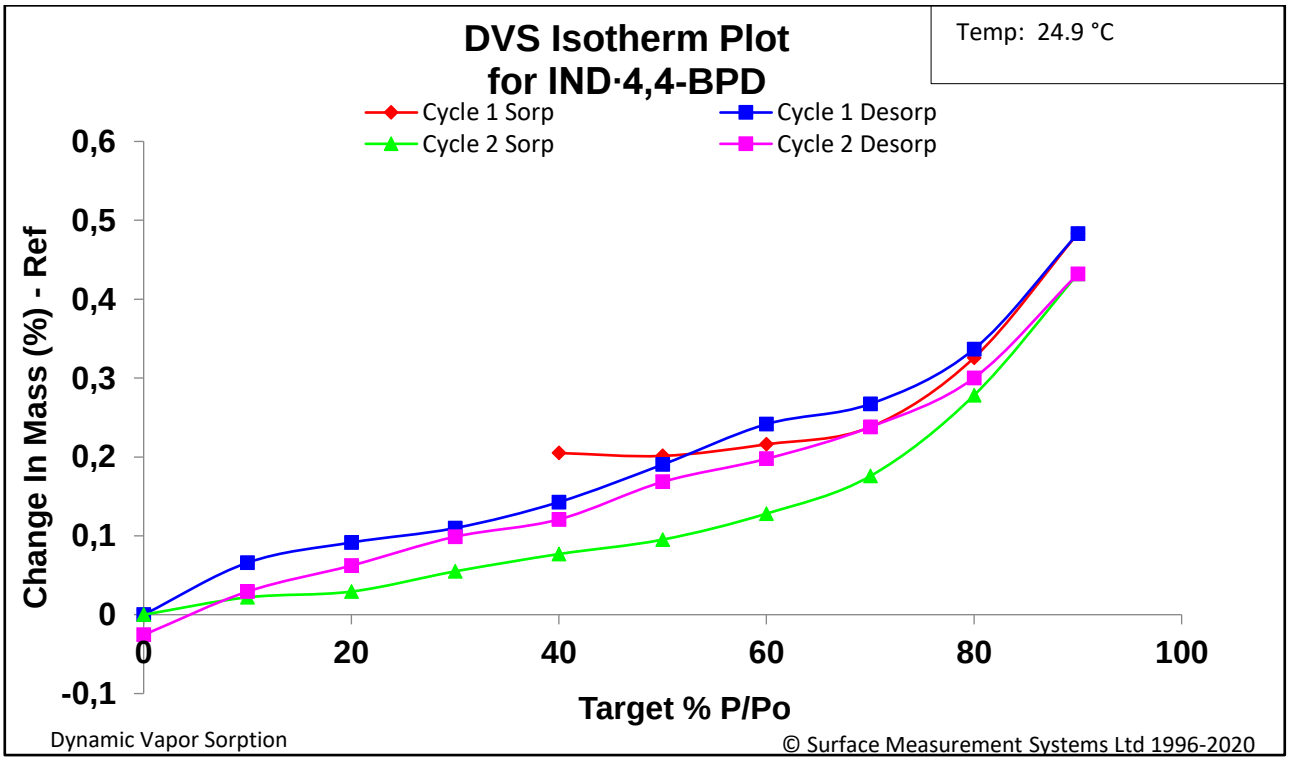

Figure 26: This is a dynamic vapor sorption (DVS) isotherm plot for IND·4,4-BPD. The graph shows how the mass change depending on the relative humidity P/P_0, as the relative humidity (RH) changes stepwise with 10% steps in two cycles. The first cycle includes sorption from 40% RH to 90% RH and desorption from 90% RH to 0% RH. The second cycle includes sorption from 0% RH to 90% RH, and desorption from 90% RH to 0% RH. IND·4,4-BPD is not hygroscopic.

Discussion

Searches for cocrystals of trifluoperazine dihydrochloride were attempted using promising coformers such as oxalic acid, gallic acid and etidronic acid monohydrate. However, no cocrystals have been achieved. The reason for this may be that the computational screening using COSMOtherm was performed on free base trifluoperazine instead of the actual compound itself which is trifluoperazine dihydrochloride. The assumption was that the free base trifluoperazine and the chloride anion would dissociate, allowing for interaction between the coformer and free base trifluoperazine. If the ionic bond between the chloride anion and free base trifluoperazine cannot be broken, the only way to create a new form is through polymorphism or through the formation of a three-component (ternary) multicomponent crystal. No cocrystal of trifluoperazine was discovered in this study, which may be due to the ionic bond between trifluoperazine and the chloride anion. However, **$TFP^{2+}\cdot 2Cl^{-}\cdot 2MeOH$** was reported in this study. This crystal was found in an unsuccessful attempt of growing cocrystals of trifluoperazine and oxalic acid (1:1) through solvent evaporation method. A similar experiment in acetonitrile also yielded a new acetonitrile solvate, $TFP^{2+}\cdot 2Cl^{-}\cdot 2ACN$, although the structure cannot be completely determined. This study recommends further structural characterization of the acetonitrile solvate. The finding of solvates may suggest that virtual cocrystal screening might have overestimated the likelihood of cocrystal formation and does not take account of solvent interaction. Interestingly, the bulk powder resulting from trifluoperazine 2HCl in isothermal slurry conversion with methanol does not match with the simulated PXRD pattern of the solvate salt **$TFP^{2+}\cdot 2Cl^{-}\cdot 2MeOH$**. This may suggest that there are different underlying crystallization mechanisms between slow evaporation which yield single crystals of a solvate salt and isothermal slurry conversion which did not create that solvate salt. To overcome the strong interaction associated with the chloride anion in trifluoperazine dihydrochloride, an anion exchange reaction with acesulfame K and Na saccharin was attempted. However, this attempt was not successful.

A search for cocrystals of indapamide was attempted through the growing of single crystals, using coformers which were promising according to computational and experimental cocrystal screening. This resulted in successful formation of the cocrystal **IND·4,4-BPD**, which was confirmed by single crystal structure analysis. Characterization through DVS shows that this cocrystal is less hygroscopic than the parent drug and much less hygroscopic than the coformer. The hygroscopicity change is due to the change in crystalline structure. If the hygroscopicity of the cocrystal depends more on the hygroscopicity of its components, the hygroscopicity of the cocrystal would be expected to be in between the hygroscopicity of the API and the hygroscopicity of the coformer. This is not the case here, as the cocrystal has lower hygroscopicity than both its API and coformer. Reduced hygroscopicity in this cocrystal is possibly caused by closure of potential hydrogen bonding sites by cocrystallization which doesn't occur in the parent drug. Further investigation by analyzing the difference of crystal structure between indapamide and cocrystal is therefore recommended. The lowered hygroscopicity in the formation of the cocrystal is important as uptake of water can alter physicochemical properties of a pharmaceutical solid. Uptake of water due to hygroscopicity can cause issues in manufacturing and storage and affect product performance. Characterization through TGA shows that the cocrystal **IND·4,4-BPD** is thermally stable until about 156°C. This temperature is well above the storage temperature for any pharmaceutical product, which means the cocrystal would be suitable for development.

With more time, and access to a better SCXRD diffractometer, combinations that resulted in single crystals of too low quality to be analyzed with the SCXRD diffractometers used for this thesis would be recreated and reanalyzed. The temperature used for attempting cocrystallization would be increased, as heightened temperature might aid in overcoming activation energy in forming a cocrystal. A further attempt to create and characterize **$TFP^{2+}\cdot 2Cl^{-}\cdot 2MeOH$** powder

would be undertaken as would an attempt to resolve the structure of $TFP^{2+}\cdot 2Cl^{-}\cdot 2ACN$ and refine the structure of the new cocrystal hydrate **IMIA·2NDS·2H_2O** which included the decomposed indapamide.

Overall the aim of finding new multicomponent crystals including the APIs trifluoperazine and indapamide was fulfilled. A cocrystal including indapamide was discovered, with lower hygroscopicity than both the API and the coformer. A new trifluoperazine salt solvate was also found. In addition to this the previously unknown molecule **N-isopropyl-2-methyl-indolin-1-amine** (IMIA) was discovered, along with a cocrystal hydrate including this new molecule.

Conclusion

During the attempt to find multicomponent crystals including either of the APIs trifluoperazine and indapamide, two new crystal structures were discovered. They are the trifluoperazine salt solvate of **TFP^{2+}·$2Cl^{-}$·2MeOH** and the cocrystal hydrate **IMIA·2NDS·$2H_2O$**, where IMIA is **N-isopropyl-2-methyl-indolin-1-amine**. The cocrystal **IND·4,4-BPD** was also discovered using the method described in this thesis, but was previously known. However, characterization showed **IND·4,4-BPD** to be considerably less hygroscopic than indapamide and much less hygroscopic than 4,4-bipyridine. This is an improvement as uptake of water can alter physicochemical properties of pharmaceutical solids and negatively affect their product performance. The improvement in hygroscopicity is due to the difference in crystalline structure between the API and the cocrystal.

Bibliography

Ann W. Newman, S. M.-E. (2008). Characterization of the "Hygroscopic" Properties of Active Pharmaceutical Ingredients. *Journal of Pharmaceutical Sciences*, vol. 97, no. 3.

AstraZeneca. (2022). AstraZeneca Internal Procedure.

Biovia. (2020, September 3). *Drug Development Complemented: COSMO-RS Applications to Solubility & Cocrystals.* Retrieved from Youtube: https://www.youtube.com/watch?app=desktop&v=enxKpR29Roc

Christer B. Aakeröy, A. S. (2018). *Co-crystals: Preparation, Characterization and Applications.* The Royal Society of Chemistry.

Clark, C. M. (2022, June). *Single Crystal Structure Refinement (SREF).* Retrieved from Geochemical Instrumentation and Analysis: https://serc.carleton.edu/research_education/geochemsheets/SREF.html

Dabing Chen, R. S. (2009). *Hygroscopicity of Pharamceutical Crystals.* University of Minnesota.

Dutrow, C. C. (2022, June). *Single-crystal X-ray Diffraction.* Retrieved from Geochemical Instrumentation and Analysis: https://serc.carleton.edu/research_education/geochemsheets/techniques/SXD.html

Hofmann, P. (2015). *Solid State Physics: An Introduction.* Weinheim: Wiley-VCH.

Karimi-Jafari, e. a. (2018). Creating Cocrystals: A Review of Pharmaceutical Cocrystal Preparation Routes and Applications. *Crystal Growth & Design*, 6370-6387. Retrieved from Crystal Growth & Design: https://pubs.acs.org/doi/pdf/10.1021/acs.cgd.8b00933

Kennepohl, D. (2022, October). *Nucleophilic addition of amines: Imine and enamine formation*. Retrieved from Organic Chemistry II: https://courses.lumenlearning.com/suny-potsdam-organicchemistry2/chapter/21-4-imine-formation/

Loschen, C. &. (2013, November). *COSMOtherm as a Valuable Tool for Cocrystal Screening and Development*. Retrieved from ResearchGate:

https://www.researchgate.net/publication/258389141_COSMOtherm_as_a_Valuable_Tool_for_Cocrystal_Screening_and_Development

Merck. (2022, March). *Advanced Search.* Retrieved from Merck: https://www.sigmaaldrich.com/SE/en/search

National Center for Biotechnology Information. (2022a, February). *Trifluoperazine*. Retrieved from PubChem: https://pubchem.ncbi.nlm.nih.gov/compound/Trifluoperazine

National Center for Biotechnology Information. (2022b, February). *Compound Summary Indapamide*. Retrieved from PubChem: https://pubchem.ncbi.nlm.nih.gov/compound/3702

Norberg, S. (2020). *User instructions for Thermogravimetric Analyzer.* AstraZeneca.

polymorphism. (2009, May 6). Retrieved from Encyclopaedia Britannica: https://www.britannica.com/science/polymorphism-crystals

PubChem. (2022). *4,4-bipyridine*. Retrieved from National Center for Biotechnology Information: https://pubchem.ncbi.nlm.nih.gov/compound/4_4_-Bipyridine#section=Melting-Point

Rigaku OD. (2022). CrysAlis Pro.

Schroeder, D. V. (2000). *An Introduction to Thermal Physics.* Addison Wesley Longman.

Sheldrick. (2015). *Crystal structure refinement with SHELXL.* Acta Crystallogr C Struct Chem.

Speakman, S. A. (2022, June). *Basics of X-Ray Powder Diffraction.* Retrieved from X-ray Diffraction Shared Experimental Facility: http://prism.mit.edu/xray/oldsite/Basics%20of%20X-Ray%20Powder%20Diffraction.pdf

TA Instruments. (2022, March 13). *MODULATED DSC: HOW DOES IT WORK?* Retrieved from http://www.tainstruments.com/pdf/literature/MDSC.pdf

Vasudha Murikipudi, P. G. (2013). Efficient throughput method for hygroscopicity classification of active and inactive pharmaceutical ingredient by water vapor sorption analysis. *Journal of Pharmaceutucal Development and Technology*, 8(2):348--358.

Zhou Y, e. a. (2018). *The Effects of Polymorphism on Physicochemical Properties and Pharmacodynamics of Solid Drugs*. Retrieved from National Library of Medicine: https://pubmed.ncbi.nlm.nih.gov/29766778/

Appendix

A. Some PXRD Diffractograms for Experimental Cocrystal Screening

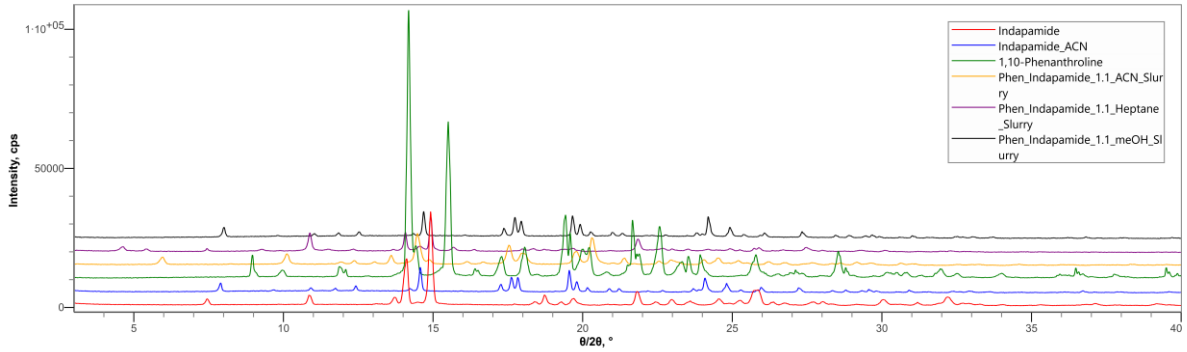

Figure 26: PXRD patterns of indapamide mixed with 1,10-phenanthroline in isothermal slurry conversion for more than 24 hours using the solvents heptane, methanol and ACN. These patterns can be compared with the PXRD patterns of pure indapamide and pure 1,10-phenanthroline, as well as the PXRD pattern for indapamide which has been mixed with ACN in isothermal slurry conversion for more than 24 hours.

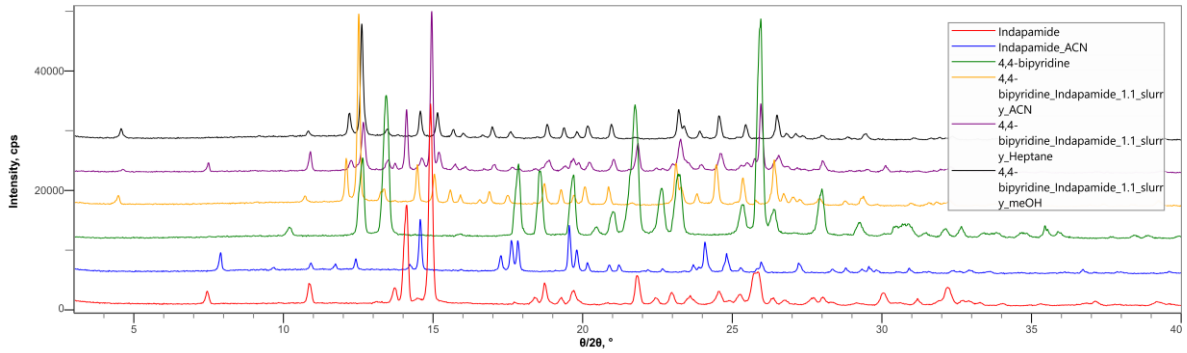

Figure 27: PXRD patterns of indapamide mixed with 4,4-bipyridine in isothermal slurry conversion for more than 24 hours using the solvents heptane, methanol and ACN. These patterns can be compared with the PXRD patterns of pure indapamide and pure 4,4-bipyridine, as well as the PXRD pattern for indapamide which has been mixed with ACN in isothermal slurry conversion for more than 24 hours.

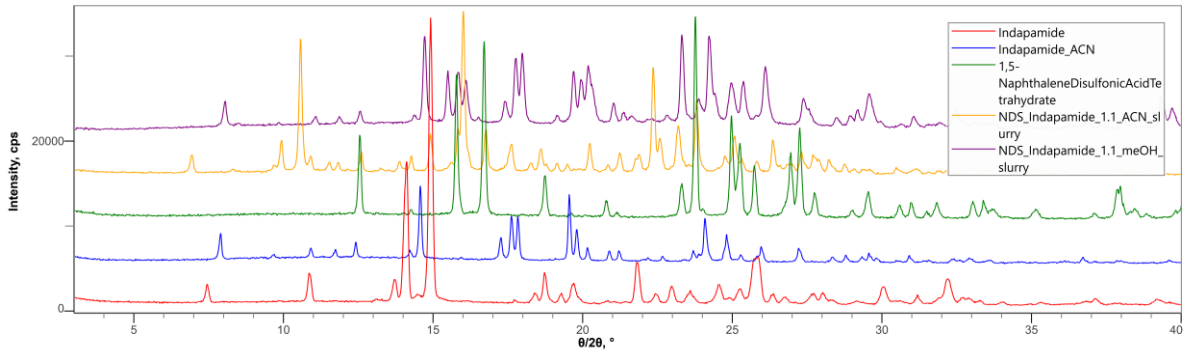

Figure 28: PXRD patterns of indapamide mixed with 1,5-Naphthalenedisulfonic acid tetrahydrate (NDS) in isothermal slurry conversion for more than 24 hours using the solvents methanol and ACN. These patterns can be compared with the PXRD patterns of pure indapamide and pure NDS, as well as the PXRD pattern for indapamide which has been mixed with ACN in isothermal slurry conversion for more than 24 hours.

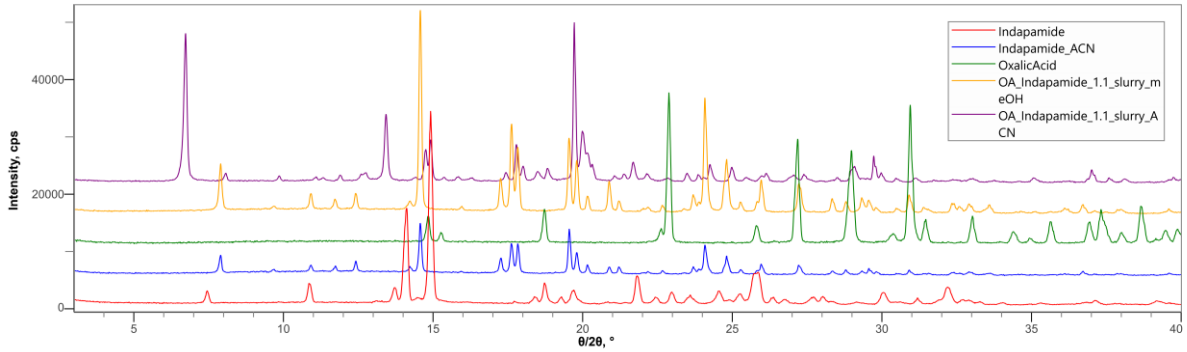

Figure 29: PXRD patterns of indapamide mixed with oxalic acid (OA) in isothermal slurry conversion for more than 24 hours using the solvents methanol and ACN. These patterns can be compared with the PXRD patterns of pure indapamide and pure NDS, as well as the PXRD pattern for indapamide which has been mixed with ACN in isothermal slurry conversion for more than 24 hours.